Preparation and Properties of Ni-SiC Functionally Gradient Material by a Powder Metallurgy Route

by

BIJAY BHUJBAL

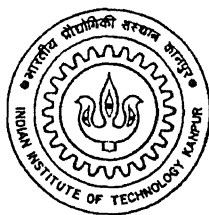## DEPARTMENT OF MATERIALS & METALLURGICAL ENGINEERING
INDIAN INSTITUTE OF TECHNOLOGY KANPUR
April, 1999

Preparation and Properties of Ni-SiC Functionally Gradient Material by a Powder Metallurgy Route

A Thesis Submitted

in Partial Fulfilment of the Requirements

for the Degree of

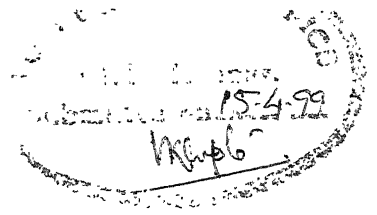MASTER OF TECHNOLOGY

by

BIJAY BHUJBAL

to the

DEPARTMENT OF MATERIALS & METALLURGICAL

ENGINEERING

INDIAN INSTITUTE OF TECHNOLOGY KANPUR

APRIL, 1999

CERTIFICATE

It is certified that the work contained in the thesis entitled **"PREPARATION AND PROPERTIES OF Ni-SiC FUNCTIONALLY GRADIENT MATERIAL BY A POWDER METALLURGY ROUTE"** by Bijay Bhujbal, has been carried out under my supervision and that this work has not been submitted elsewhere for a degree.

Dr. R.K. Dube,
Professor,
Department of Materials and
Metallurgical Engineering,
Indian Institute of Technology,
Kanpur.   208016

April, 1999.

ABSTRACT

Ni-SiC FGM compacts were prepared by hot pressing the powders. Subsequently these compacts were sintered for different time and temperature. The physical and mechanical properties together with the microstructure of the sintered hot pressed compacts are studied. It has been shown that Ni-SiC FGM compacts consisting of four layers having composition in successive layers as 100% Ni, 90% Ni-10% SiC, 75% Ni-25% SiC and 50% Ni-50% SiC can successfully be formed by hot pressing at 950 $°C$, followed by sintering at 1150$°C$. The FGM compacts have about 95% of the theoretical density when the hot pressing was done at 950$°C$ for 120 min. followed by sintering at 1150$°C$ for 120 min.. The nickel concentration profile of the hot pressed and sintered Ni-SiC FGM compact suggests that no noticeable homogenisation of the Ni-SiC FGM compacts has taken place after sintering at 1150$°C$ for 120 min.

ACKNOWLEDGEMENTS

Contents

List of Figures

List of Tables

Chapter 1

Introduction

Functionally Gradient Materials (FGM) are those materials which exhibit a progressive change in composition, structure and properties as a function of position within the material. A typical FGM is the functionally graded heat resistant material, as shown in Fig.1.1[1].
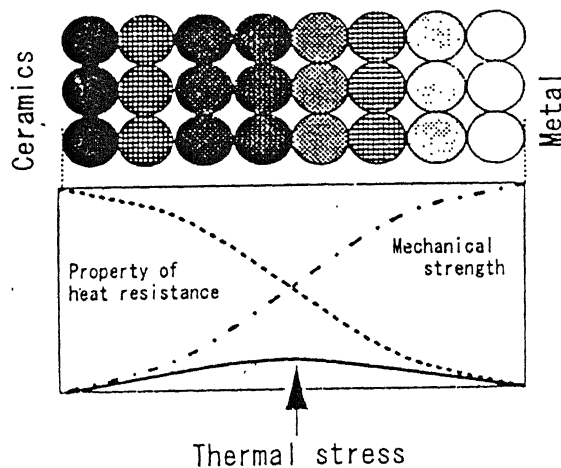
Figure 1.1: Functionally graded heat resistant ceramic-metal joint

This comprises a ceramic material providing excellent heat resistant properties and

a metallic material providing both high mechanical strength and thermal conductivity. The ceramic material on one side is gradually modified to the metallic material on the other. This material combines the functionality of both ceramic and metal, and reduces the magnitude of thermal stresses originating from the difference of thermal expansion coefficient between the two materials. The additional functionality of this material is, therefore, the ability to relieve thermal stress.

FGM materials are characterized by a nonlinear, three dimensional distribution of phases and corresponding properties. They are distinguished from isotropic materials by gradients of composition, phase distribution, porosity, texture and related properties such as hardness, density, thermal conductivity, etc. These gradients are quantitatively controlled in order to achieve improvement in properties of the product[2, 3].

Functionally gradient materials are different from conventional (non-graded) materials in the following ways:[4, 5]

(a) During design of the FGM the optimal gradient of a certain property and/or composition must be considered. It is not possible to specify a gradient composition in the material without being aware of the exact requirements of the intended application of the components, and its working conditions.

(b) Usual techniques, such as standard thermal conductivity measurements make no sense for FGM, because the results will depend on the way the specimen is located or cut from the whole part. For other properties the test procedure usually has to be modified. For example, the fracture modes in FGM may change from brittle to ductile with changing microstructure, causing changes on the microscopic scale such as crack initiation and propagation and fatigue resistance.

Application of FGMs

Some important applications of FGMs are given below.

1. Joining Media

Because of their potential for reducing thermal stress, FGMs have been investigated for joining metals to ceramics (Metal/FGM/Ceramic) and both metals and ceramics to FGMs (metal/FGM, ceramic/FGM).

It has been studied that nickel is joined to MgO with an FGM filler of Ni-NiO with good adhesion at the joining interfaces. The joined composite, Ni/Ni-NiO(FGM)/MgO was formed by heating at $1300°C$ at atmospheric pressure in air. A composition gradient was formed between the nickel and the solid solution.

An FGM filler of Ni-MgO was similarly used to join Ni to MgO, forming Ni/ Ni-MgO(FGM)/MgO. The fracture strength (three-point bending test) of the joints formed using the FGM Ni-NiO (72-128 MPa) and FGM Ni-MgO (110 MPa) was higher than when Ni was directly jointed to MgO (30-60 MPa). Iron was also successfully jointed to AlN via an FGM of Al-AlN by containing the aluminum surface of the FGM with the iron and heating at $650°C$ for 48 hours in flowing argon. The microhardness of the Al-rich zone in the FGM was harder than pure aluminum[6].

2. Shuttle Thermal Insulation

A thermal protection FGM type tile developed for the space shuttle is more efficient and less costly than tiles currently being used. This tile, is known as Toughened Uni-Piece Fibrous Insulation (TUFI), is a low density composite thermal insulation. It is the first FGM composite where the density of the material varies from high at the outer surfaces to low in the interior insulation.

The current tiles are a rigid glass-fibre composite and are about 93% air, with a thin glass coating on top. The Reaction-Cured Glass (RCG) coating is physically much like windows glass and is only about 0.03 mm thick. Because the coating gets little support from the underlying tile, it cracks or chips easily. Unlike RCG, TUFI permeates the pores nearer the surface of the insulation material. This supports and reinforces the outer surface, which makes the surface material less subject to impact damage[7].

3. Future Shuttle and Aerospace Planes

Several study programs are underway to establish material design technology for creating complex-shaped FGMs and introducing FGM designs into the fuselage and engines of a reusable shuttle plane and other supersonic planes.

In the development of large FGM test samples, a number of basic shapes have been adopted to promote the use of FGMs in the space planes fuselage and engines. These shapes include a semi spherical shape that is required to create FGMs for use in the planes nose cone section, a hollow cylinder to make FGMs for application in the front edges of the wings and engines, and a square plate to manufacture FGMs for use in other sections.

4. Dental Implant

Researchers at Tokyo Medical and Dental University[8] have developed a dental implant (artificial tooth root) using FGM. The material consists of primarily of apatite that has a high biocompatibility with bone and titanium that provides the necessary strength.

Implants are produced today using a ceramic (apatite) and metals such as titanium. Apatite is biocompatible with the bone but lacks strength and is brittle, while titanium has a greater strength than natural tooth but has less affinity with bone. Thus by taking advantages of both these materials an implant is made of apatite and titanium.

FGM specimens were formed with the content changing gradually from pure titanium at one end to 9% ceramic at the other end.

The prototype implant was used in various strength tests. When apatite and titanium were mixed at ratio of 1:9, the compressive strength was about 500 MPa. When tests were conducted on implants made only of apatite, the compressive and flexural strengths were only a few dozen MPa.

5. Building Material

Takahashi et al.[9] has successfully developed FGM with moisture absorption and release functions made by step wise or continuously changing the composition of two components-a zeolite or ligneous material-based humidity-conditioning material, capable of absorbing and releasing moisture, and calcium silicate-based concrete. This FGM can absorb a maximum of approximately 2.5 times more moisture, and is particularly good in its initial response to a humidity increase or decrease.

In addition the new material hardly changes its dimensions by expansion or contraction due to humidity; and it is strong, fire proof, frost damage resistant, and quite amenable to shape forming from flat board to curved corner material. As a building material, this material with a gradient moisture conditioning property from its outer wall to inner wall, could eliminate extra construction steps for faster completion.

Chapter 2

Literature Review of Methods of Manufacturing Functionally Gradient Materials

FGMs are now attracting attention worldwide as new materials in which locally different functions can be added to a single material by continuously changing dispersion phase density, kinds or structure from one side of the material to the other, or by changing them locally to alter its characteristics. Though the term "functionally gradient material" is indisputably mouthful, talking about these new-fangled materials has proven much easier, than producing them.

Functionally gradient materials can be produced by a variety of methods. Some important methods are described in the subsequent sections.

2.1 Laser Alloying and Cladding

In the field of high power laser processing, the techniques of surface alloying, cladding and particle injection provides possible routes for producing certain types of FGMs. To produce gradients normal to the substrate surface, successive fully overlapping alloyed and clad layers can be deposited using powder feed mixtures with increasing proportions of one or more components to provide composition range. Control of the dilution from substrate influences the composition of the first layer and in succeeding deposits the dilution from each underlying layer is critical. The technique produces a series of layers of essentially discrete composition rather than a graded composition range .

Individual laser tracks are relatively narrow, typically a few millimeters, and the production of FGM layers over a substantial surface area necessitates partial overlapping of a series of tracks in the horizontal direction, followed by super imposition of another similar series of tracks to achieve the vertical gradient. The compositional and structural gradients are made more complex by this pattern of horizontal and vertical overlapping.

Abboud and his associates[10] used two approaches in processing FGMs materials: (1)surface alloying of a near-alpha-Ti alloy substrate using a powder feed of Al and (2)cladding on to a commercial purity (CP) Ti substrate using powder mixtures of Al with Ti-6Al-4V alloy. They found that cladding involving low dilutions provided a better approach to producing several discrete layers of increasing Al content than did alloying which is associated with higher dilutions. This cladding technique used powder mixtures of Al and Ti-6Al-4V (wt%) alloy which involved low dilutions and allowed several layers of discrete composition to be produced having Al contents in the range from 10.5 wt% (approximately 18 at%) to 34.5 wt% (approximately 48 at%).

Jasim, Rawlings and West[11] applied a technique of injection with a powder feed of a mixture metal-ceramic which combines the processes of laser alloying, cladding and

injection to study the feasibility of using a continuous-wave CO_2 laser to produce an FGM.
A 2-KW CO_2 laser was used to produce, on a nickel alloy substrate, single alloy/clad tracks
and three totally overlapping clad tracks using powder mixtures of Al-10 wt% SiC, Al-30
wt% SiC and Al-50 wt% SiC, respectively.

Jasim, Rawlings and West[11] have also showed that an FGM can be produced by
laser processing of Al-SiC powder mixtures on a nickel alloy substrate (IN 625) and that
three successive tracks can be deposited to give a wide range of compositions progressing
from the inner to the outer regions. However, the accompanying changes in microstructure
through the 3 millimeter thick FGM were not fully satisfactory. In particular, it was found
to be difficult to retain a significant proportion of the SiC_p other than in the final layer of
the FGM. Furthermore, because of the number of alloying additions in the substrate, the
moicrostructures were complex and difficult to interpret and the results show the need for
detailed consideration of the constituents when designing a multicomponent system.

2.2   Chemical Vapor Deposition(CVD)

Chemical Vapor Deposition is a process route similar to physical vapor deposition. In this
process the composition of the condensed layer is controlled by process variables such as
temperature and gas composition. By controlling the CVD conditions, the microstructure
of the FGM coatings can be changed from dense to porous. The porous structures were
found to resist both delamination and crack propagation and the researchers concluded
that by controlling the microstructure of the FGMs, both their thermal barrier and thermal
fatigue properties can be controlled.

Kude[12] deposited an FGM on a complex shape by CVD of a six-step SiC FGM on
carbon fibers, on a cylindrical graphite tube, and on a graphite plate. The source gases
for the coatings were methane (CH_4) for the carbon and silicon tetrachloride ($SiCl_4$) and

methane for the SiC. The carbon content in the deposit was changed by changing the

molar ratio of the two gases; i.e, changing the ratio of Si/C in the gas phase changes the

ratio of $C/(SiC + C)$ in the deposit. The FGM composite with an FGM SiC/C CVD

coatings has been tested for thermal fatigue in a rocket combustion environment with

excellent results.

2.3 Electrophoretic Deposition

Electrophoretic deposition is a process whereby particles are deposited from a suspension

on to a shaped electrode of opposite charge, on application of a dc electric field. The rate of

deposition is controllable via the deposition current density and suspension concentration

and it can be very fast.

This process is a combination of two processes, electrophoresis and deposition. Elec-

trophoresis is the motion of charged particles in a suspension under the influence of an

electric field gradient. The second process is deposition,i.e. the coagulation of particles

into a dense mass.

Dealing first with electrostatic stability, when a particle is submerged in a liquid, the

electrochemical nature of its surface changes, ions leave or adsorb and the particle assumes

a surface charge. This surface charge is balanced by an increase of oppositely charged ions

(counter-ions) and a decrease of co-ion concentration in the vicinity of the particle in the

liquid. This charged atmosphere around a particle is called the "diffuse-doubled layer" or

"lyosphere". When a particle moves, some of the ions in the diffused double-layer region

"shear off" and the residual potential at the shear-plane is called "τ-potential". The higher

the potential, the more stable is the suspension against coagulation (coagulation is due to

the Van der Walls attraction forces which dominate on very close particle approach.

By EPD it is possible to synthesize step FGMs and continuous profile of the FGM can be

controlled by deposition current density, second component flow rate, suspension concentration etc. Step and continuous profile Al_2O_3/YSZ and continuous profile $Al_2O_3/MoSi_2$, Al_2O_3/Ni and YSZ/Ni is synthesize by EPD.

For synthesis of Al_2O_3/YSZ, the starting materials were 3 m/o Y_2O_3-Stabilized Zirconia (YSZ), Al_2O_3, $MoSi_2$ and Ni. Suspension are prepared by vibromilling in absolute ethyl alcohol with pH values controlled to introduce suitable charge (+ve or -ve) in the suspended particles. The details of suspension preparation is given in the Table1.1.

Materials	Particle Size (μm)	Suspending Media	Dispersent	pH
Al_2O_3	~0.25	Ethanol	-	3.5-4.0
YSZ	~0.2	Ethanol	-	3.5-4.0
$MoSi_2$	-325 mesh	Ethanol	Boehmite	-
Ni	~0.7	Ethanol	$Al(NO_3)_3$	-

Table 2.1: Details of Suspension Preparation for Electrophoretic Deposition

Deposition was started with a YSZ suspension, and a stream of Al_2O_3 suspension was slowly injected into the bottom of the EPD bath by syringe pump. Al_2O_3 and YSZ mixed at the bottom of the bath. The mixing area was shielded from the depositing cathode by a plate. The profile of Al_2O_3 can be precisely controlled by, the deposition current density, the rate of pumping of the Al_2O_3 suspension into the YSZ and the concentration of the suspension. After deposition, the deposit was dried, the green compact removed and sintered in air at $1525°C$ for 6 hour[13].

The compositional gradient across the Al_2O_3/YSZ FGM was characterized by through-the-thickness variation of composition, hardness, and indention fracture toughness.

2.4 Centrifuging

The principal idea of this method is to build up a ring with a "through-thickness gradient" by feeding a powder mix of varying composition into the centre of a centrifuge, so that

it will be projected towards the inner surface of the outer wall of the centrifuge vessel.

The centrifuge for Powder Metallurgy gradient ring preparation is shown in Fig. 2.1. This
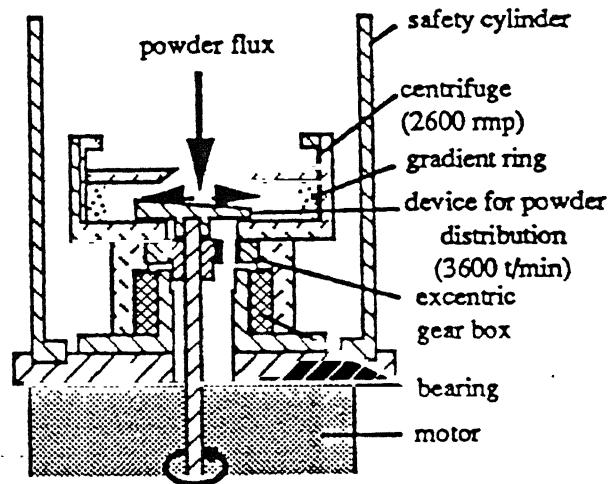
Figure 2.1: Centrifuge for Powder Metallurgy ring preparation

produces the desired concentration profile in the ring, taking into account the shrinkage

during compaction and sintering. For this purpose, the different powder components are

stored in three vertical cylinders. The powders are collected on a planner platen where they

are premixed and transferred. The mixture falls on a disk type accelerator which is coupled

to centrifuge proper, projecting it towards the centrifuge wall. Schematic presentation of

the centrifugal Powder Metallurgy process is shown in Fig. 2.2. This gradient process

is to create "soft" gradients and to avoid abrupt transitions of composition. However,

there is risk of demixing of heavy and light (or of large and small) powder particles due to

centrifugal force. In fact, the friction between the individual powder particles doesn't allow

for "diffusive" motions. The ring is stabilized within the rotating centrifuge by injection of

a paraffin type binder phase. After sometime, when the binder becomes sufficiently hard,

the centrifuge can be brought to halt so that the ring can be taken out [14].
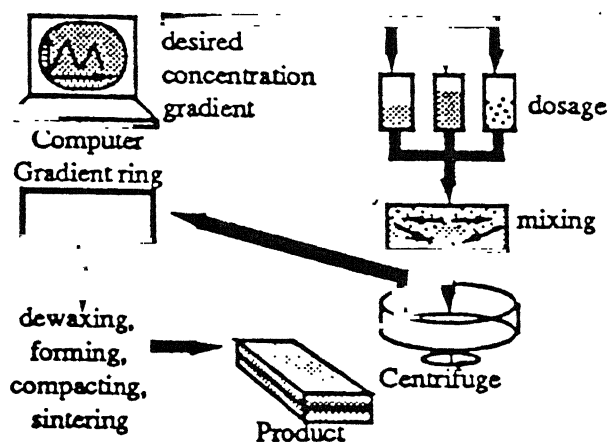
Figure 2.2: Schematic presentation of the centrifugal Powder Metallurgy process

2.5 Galvanoforming

The powder metallurgical fabrication route is not suitable for the preparation of thin

gradient foils for micro technical applications, since the specimen thickness will become

comparable to the average powder grain size. For this reason, Galvanoforming has been

examined as an alternative method. For this an experimental device has been developed

with individual anodes for each of the alloying elements, controlled by individual galvano-

static circuits. The individual current densities are enforced by a piloting computer. The

anodes form a circular array (connected to the current source by sliding contacts). The

cathode covers the outer wall of the electrolytic cell which has the shape of a flat cylinder,

it consists either of metallised plastic or of stainless steel foil, in the latter case, the passive

layer permits easy separation of the gradient foil from its substrate, while the anodes rotate

concentrically of the individual anodes and receives a deposit of one element at a time.

These nanodeposits are building up periodic layers, the periodicity of which is of the order

of 0.01 μm approximately. The whole arrangement is shown in Fig. 2.3.
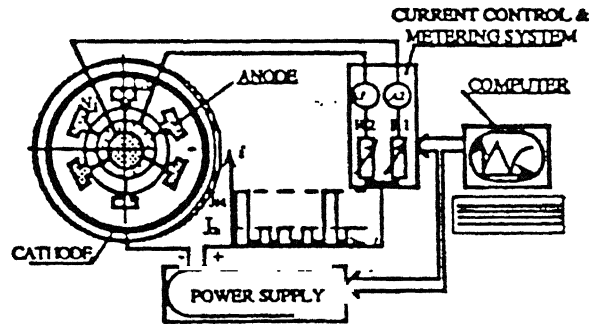
Figure 2.3: Schematic presentation of Galvanoforming apparatus

Instead of galvanostatic technique, a potentiostatic one may be used which controls the distribution of the two metal components by means of the cathodic potential drop. The anodes serve primarily to maintain the electrolyte at constant composition. Pulse plating technique may be applied either to deposit alternate layers of different composition or to improve the structural quality of the deposited metal.

As an additional possibility, inorganic powders (alumina, SiC) may be injected as fine emulsions into the electrolyte in order to form particle-dispersion hardened layers by occlusion in the graded foil. This process starts by adhesion of individual particles to the surface, some of which will be overgrown by deposition of metal, thus forming the dispersion. The number of particles captured by the growing surface depends on the particle density within the electrolyte phase, on current density and on agitation of the liquid. It is possible to fabricate layers with a predetermined particle density [14].

2.6 Self Propagating High-Temperature Synthesis/ Hot Isostatic Pressing (SHS/HIP)

Miyamoto and his associates [15, 16] at Osaka University have prepared a symmetrical $Cr_3C_2 - Ni - Cr_3C_2$ FGM structure from Cr_3C_2 and Ni by SHS/HIP method using Si fuel (Fig.2.4). The HIP was carried out in nitrogen atmosphere at 100 MPa. The Si fuel burns in nitrogen at pressure > 3 MPa and forms Si_3N_4. The Si fuel makes the SHS/HIP process safer and more economical. Using thermite pellets which are placed at desired points in a chemical oven and reacted at temperature $< 1000°C$, the need for an electrical ignition system is eliminated.

The SHS/HIP method using Si fuel can produce dense materials instantaneously due to the high heat generation of silicon nitridation in the advantage of energy saving.

The $Cr_3C_2 - Ni - Cr_3C_2$ FGM structure had residual compressive stresses at the surface. As a result, the material had a bending strength of 85 Kg/mm_2, which is 50-60% higher than the FGM structure produced by conventional sintering process. The material was also found to have improved fracture toughness, about 10 MPa $m^{1/2}$ at Cr_3C_2 rich surface compared with 5.3 MPa $m^{1/2}$ of the monolithic Cr_3C_2. This is believed to be due to the strong residual compressive stresses (580 MPa) induced at the surface by contraction of the Ni-rich center layer (which has a higher rate of thermal expansion than the surface), during the rapid heating and cooling in the SHS/HIP processed.

A symmetrical $Al_2O_3 - TiC - Ni - TiC - Al_2O_3$ FGM structure has also been synthesized, which is expected to have a self - repair function for passivation due to TiC oxidation at high temperatures. Feng and Moore [17] investigated the $TiB_2 - Al_2O_3 - Al$ FGM by utilising SHS as an efficient processing route for these synthesis of ceramic-metal composite system.

POWDER MIXING $Cr_3 C_2$, Ni

Powder Lamination

100% $Cr_3 C_2$, 0% Ni

75% $Cr_3 C_2$, 25% Ni

50% $Cr_3 C_2$, 50% Ni

75% $Cr_3 C_2$, 25% Ni

100% $Cr_3 C_2$, 0% Ni

CIP   200 MPa

Si Fuel   SHS/ HIP   100 MPa, N_2

FGM   30 x 5 mm
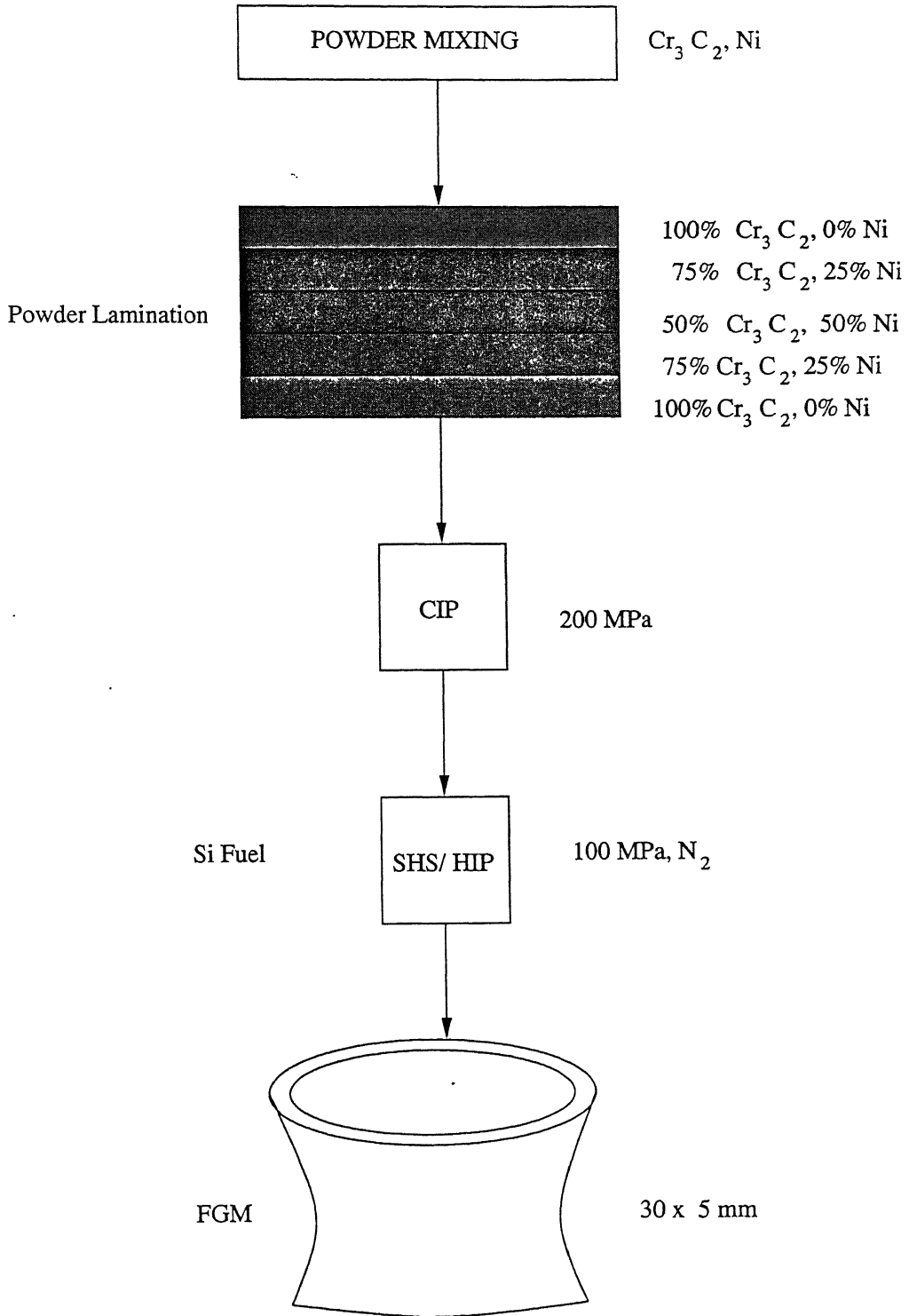
Figure 2.4: A flow diagram of the Experimental Procedure for the fabrication of the symmetrical FGM, $Cr_3C_2/Ni/Cr_3C_2$

2.7 Pulse Electric Discharge Method

A novel method of pulse electric discharge resistance consolidation with temperature gradient control has been developed by Kimura and Toda [18] for the design and fabrication of functionally graded materials. The powder processing route employed makes it possible to select combinations of constituents densification rates, controlling densification up to full density to produce nanoscaled structure. A die with specially designed outer shape makes it possible to achieve desired temperature profiles along a graded composition. A temperature differences of approximately 700 K appears over a distance of 7 mm under a current of 1400 A. The difference in temperature in a stepped die arises from the change in current density with wall thickness.The pulse discharge resistance consolidation setup involving temperature control using a stepped die is shown schematically schematically in Fig.2.5.

Kimura and Toda [18] have produced a five layered material graded from TiAl intermetallic on one side to partially stabilized Zirconia (PSZ) on the other side and having three intermediate layers having Ti-Al:PSZ compositions as 3:1; 1:1; and 1:3. The increase in temperature of the PSZ layer as a function of the temperature of the TiAl layer is shown in Fig.2.6. This structure shows full densification throughout its cross-section without any discontinuities and an increasing hardness from 650 HV at the TiAl nanocrystalline layer to 1560 HV at the PSZ layer varying according to mixture rule [19, 20, 21].
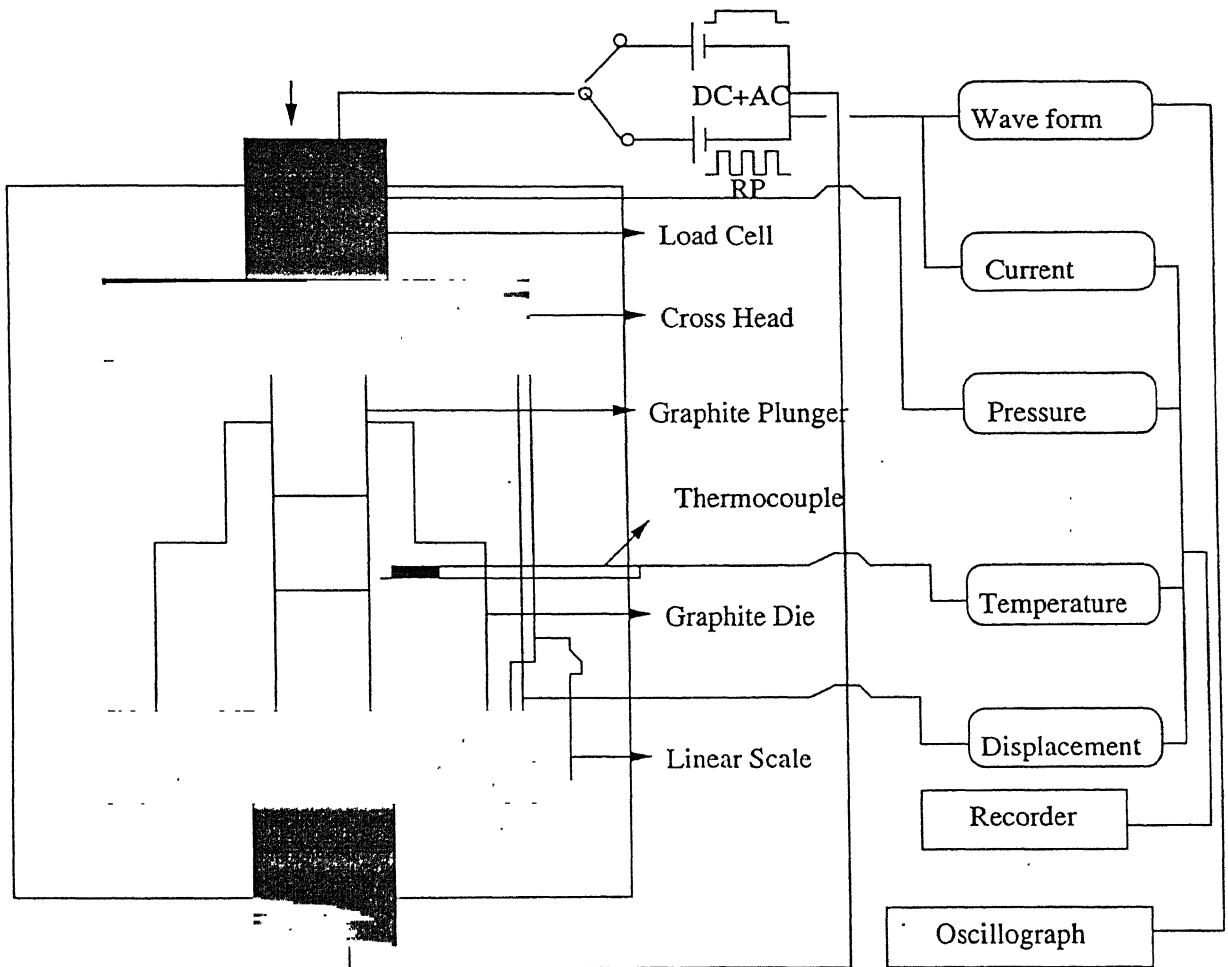
Figure 2.5: Pulse Discharge Resistance Consolidation setup involving Temperature Control using a Stepped die is shown schematically [18]
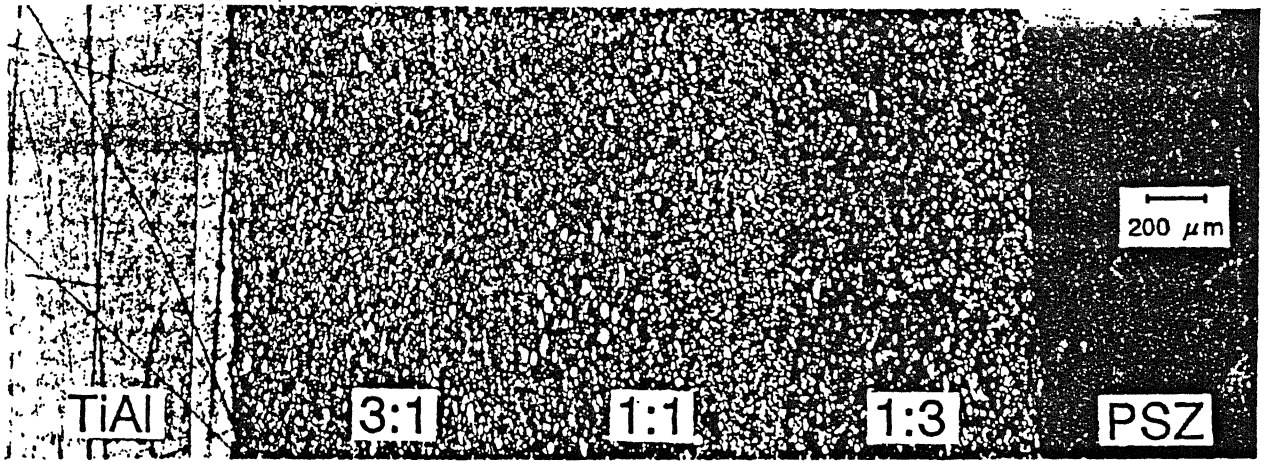
Figure 2.6: Optical micrograph of cross-section of five layer TiAl/PSZ FGM prepared under temperature profile produced by stepped die

2.8   Powder Metallurgy

Powder Metallurgy techniques can be used to make FGM products larger than those obtained by PVD/CVD. This method depends on a reliable feed mechanism for the appropriate powder mix, avoiding agglomeration of like powder particles. In principle, three-dimensional concentration distributions may be built up, layer by layer.

2.8.1   Press and Sinter/Hot Pressing Route

Components exhibiting one-dimensional concentration profile can be fabricated by vertical stacking of powder layers of varying composition within a fixed flat mould. This method involves mixing of powders according to the required composition profiles, compacting the graded powders to obtain "green" FGM compacts and subsequent sintering in a suitable atmosphere. The control of sintering shrinkage and thermal stresses are critical to obtain a graded composite with sufficient fracture strength.

Colin, et al [22] have produced multilayer graded WC-Co structures with Co content
ranging from 10% on one side to 30% on the other. The method used to produce the graded
structure containing three different layers is follows. The first layer containing WC-10%Co
was cold pressed. The second layer WC-20% Co was then poured into the die and pressed
at the same pressure. The third layer containing WC-30% Co was poured and the three
layer stack was cold pressed under a pressure of 1263 MPa. The "green" WC-Co FGM was
sintered at $1290°C$ in the solid state. Adhesion between layers was found to be good, and
mixing of the layers close to the interfaces was not observed. Microstructural examination
showed that of densification were not affected by the presence of graded structure, even
close to the interfaces between the two layers. The graded structure remained after sintering
because there was no risk of homogenization during solid state sintering. Colin, et al also
sintered the WC-Co FGM at $1353°C$, at which liquid phase sintering took place. In this
case, the sintering time had to be much shorter because densification happened much faster
with the liquid phase, and also for avoiding any homogenization of the structure.

Bishop et al [23] have investigated the preparation of Ti-Hydroxy apatite (HA) FGMs.
Mixtures of dry Ti and HA powders containing 10, 20 and 30% HA were prepared, and
poured in turn into a steel die to give the following layer arrangement: Ti, Ti-10% HA, Ti-
20% HA, Ti-30% HA and Ti. The layered powders were cold compacted at a pressure of
500 MPa for 1 min. to give a "green FGM compact". The green compacts were preheated
at 500 $°C$ for a period ranging from 30 min. to 60 min. and was subsequently hot pressed
at a pressure of 1360 MPa. The green Ti-HA FGM compact were sufficiently strong to
be handled and showed no signs of cracking. The interface between Ti and 10% HA and
between Ti -30% HA were good quality, with negligible porosity and an even distribution of
HA particles. Bishop et al claimed that the results are more encouraging and an outer layer
of high HA content. It is interesting to note that HA is bioactive and it reacts chemically
with living bone to give a strong bond that can resists high stresses. Thus, an implant

having high HA content on the outer surface becomes quickly and firmly fixed without such as screws and bone cement. It is hoped that the incorporation of HA into titanium will enhance the bonding to bone, and that by producing an FGMs this will be achieved without a significant degration in mechanical performance.

The following materials combinations has been used to prepare gradient materials: $Cu - Ni$, $Ni - Al_2O_3$, $Co - SiC$, Co-diamond, $Cu - TiB_2$, ZrO_2-stainless steel [22].

A novel method for sintering FGM compacts have been developed by Sumitomo Mining Co. Ltd. [24], which is known as spark plasma sintering process (SPS). The SPS process is a unique synthesis process, in which electrical energy introduced between the the gaps of green compact particles, and the high energy of the discharge plasma generated instantaneously is applied effectively to enable sintering or sintered bonding at a lower temperature and in shorter time compared with conventional processes. It may be regarded as a new, next generation type of sintering process that most effectively utilizes the spontaneous self-heating effect arising inside the particle specimen, as with the SHS process. FGMs based on glass and silicon, glass and stainless steel in combinations have been produced in disk form with a diameter of 2 cm and height of 1 cm. Initially a pressure of 30 atmosphere was applied to mix and solidify the powdered glass and metal without any voids. A large current of 500 A was applied intermittently at a fixed interval, after which the mixed powder was heated to $800°C$.

2.8.2 Hot Isostatic Pressing Route

Alternatively, the "green" FGM compacts can be subjected to Hot Isostatic Pressing (HIP). HIP parameters, such as temperature, pressure and time can be carefully adjusted to promote inter diffusion, but care should be taken to avoid large scale reactions that may lead to unwanted phases and degradation of the starting materials.

2.8.3   Slurry Casting Route

Several different variants of Powder Metallurgy methods have been developed for making

FGM products. In one such variant, slurry or slip casting can be used for making "green"

FGM compacts, instead of conventionally used die compaction of various layers of powder

mixture.   In this approach, a homogeneous and free flowing slurry from a mixture of

required powder mass and a suitable binder is prepared. The slurry is cast on a suitable

substrate and is subsequently dried. Slurry of a different composition is then deposited

on the previously dried slurry, and is subsequently dried. The process of slurry deposition

and drying continues till the last layer deposited. Finally a "green" FGM compacts having

different compositions in different layers are produced. The subsequent processing is similar

to that described earlier.

The keys to successful fabrication of FGM products by Powder Metallurgy methods

based on slurry route depend on the following factors:

1. Uniform dispersion of ceramic and metal particles in the slip,

2. Controlled layered microstructure in the green compact,

3. Avoidance of fracture of powder compacts by drying and sintering stresses.

Another key to the successful fabrication was to minimize differences in permeability and

pore radius between neighboring layers in the multilayer "green" compact and thus to

avoid fracture during drying in the ambient atmosphere.

Morinaga and his associates [25] succeeded in fabricating an $Al_2O_3 - W$ FGM using slip-

cast method. They obtained a gradient material with a continuously changing composition

by controlling the fine particle settling rate, which is dependent upon specific gravity and

grain size, in the slip cast method thickening process. When they use a thin 5% or 10%

slip density, the alumina layer and tungsten layer separated,confirming clear continuous

inclined layers. Takebe and Morinaga [26] fabricated a multilayer $ZrO_2 - Ni$ green compact

formed with a stepwise compositional gradient and sintered in argon atmosphere.

The Miyagi Institute of Technology and Makabe Co. [27] have jointly developed another

variant of Powder Metallurgy method based on slurry route, for making FGM products.

The slurry made from a mixture of the required powder mass and a suitable binder sprayed

by a supersonic nozzle on a substrate to form an even, continuous deposition, which is sub-

sequently dried. Subsequently, slurry of different composition is sprayed on the previously

sprayed and dried deposit, followed by drying. The process is continued till the last slurry

is sprayed and finally dried. The "green" FGM compacts is then sintered to produce the

final FGM products. The process provides in expensive way of making large cylindrical

deposits as well as planar deposits.

2.8.4 Route based on Liquid Phase Sintering of uniform composition green compacts

The starting material for producing FGM structures by Powder Metallurgy method is the

graded "green" FGM compacts. It is more complicated to prepare a graded "green" FGM

compact than a homogeneous and uniform composition compacts. The preparation of

"green" FGM compacts restricts the practical application of FGM. Tsuda et al [1] have

proposed an alternative approach for making FGM structures from a uniform composition

"green" compacts, by controlling the subsequent liquid phase sintering process alone. Sin-

tered hard materials, such as cemented carbide and cermet are composed of hard particles

and a metallic binder, and are manufactured by liquid phase sintering. Tsuda et al [1] have

produced a FGM structure having titanium based ceramic surface layer TiCN containing

no metal binder, a tough cemented carbonitride core containing B1 type (Ti,W) (C,N) and

WC phases, and an intermediate layer with graded composition as shown in Fig.2.7.

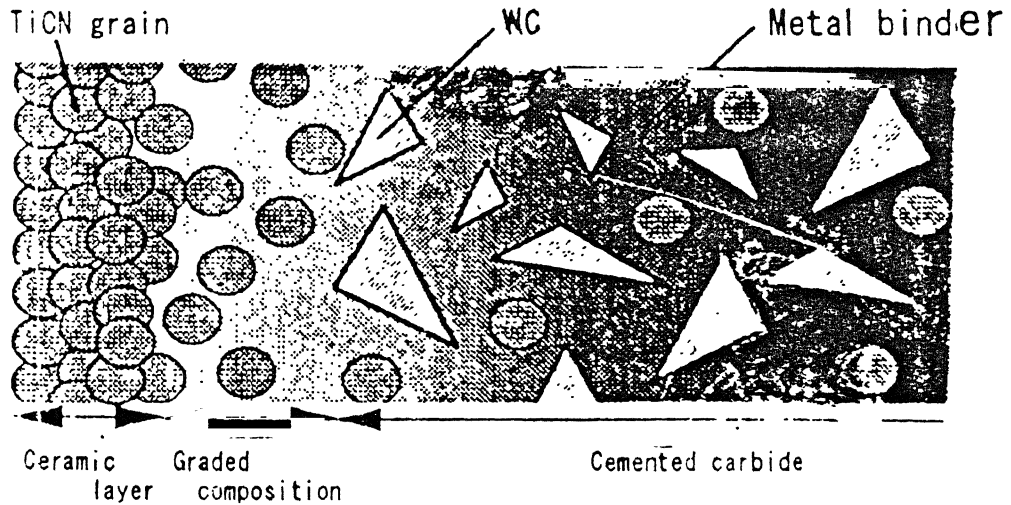Figure 2.7: Design of Functionally Graded Hard Material

Tsuda et al [1] wet mixed the powders having composition TiCN-40 WC-10 Co-5 Ni (in wt%) in a ball mill for 24 hours and press moulded into 10x10x10 mm green compacts of uniform composition at a load of 1 ton. The samples were sintered under controlled sintering temperature, atmosphere and cooling rate. However, no details of sintering parameters are given.

An EPMA line analysis of Cobalt was performed on the cross-sections. A typical distribution of the metal binder is shown in Fig.2.8. The intensity declines from the core level about 50 micro meter below the surface and there is an area near the surface containing absolutely no metal binder. The high hardness region described above is thus a binder free ceramic layer.
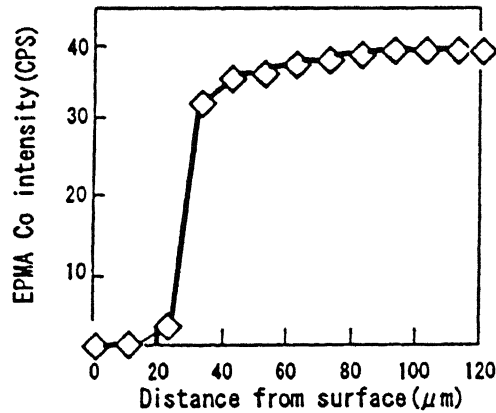
Figure 2.8: Depth profile of cobalt distribution in sintered functionally graded hard material

Tsuda et al [1] carried out toughness tests of functionally gradient sintered hard materials produced from uniform composition TiCN-40 WC-10 Co-5 Ni green compact, and the results are given in the Table 2.1. The results are also summarized in Fig.2.9. The number of impacts to tool fracture for FGM tools greater than with conventional TiCN-Ni cermet. But toughness slightly inferior to that of TiCN coated WC-Co tool because of the higher fracture toughness of the cemented carbide used for coated tool.

Cutting Conditions	Toughness test
Work Piece	SCM435(260 HB) Containing 4 Grooves
Cutting Velocity, mm/min.	150
Feed, mm/rev	0.28
Depth of cut, mm	1.5
Condition	Wet

Table 2.2: Cutting Conditions used in Toughness tests
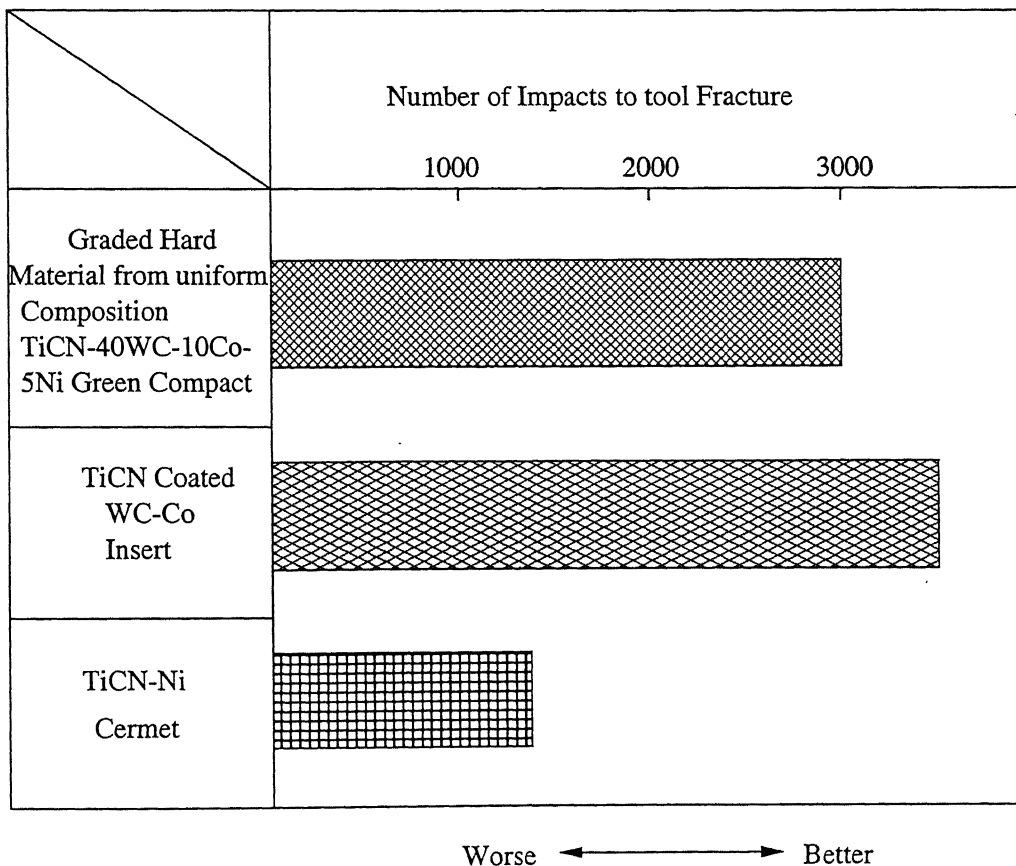
Figure 2.9: Results of Toughness Tests

Tsuda et al [1] conducted continuous wear resistance tests of functionally graded sintered hard materials using SCM435 steel under the cutting conditions shown in Table 2.2. For comparison a conventional cermet of uniform composition and a $TiC/TiCN/TiN/Al_2O_3$ multilayer CVD coated tool had approximately the same internal hardness as the FGM to adjust for the grade of the tool. The results are summarized in Fig.2.10. The wear resistance of the FGM in these conditions were approximately twice that of the conventional cermet because of the hard ceramic surface layer containing no metal binder, but slightly inferior to that of the coated tool.

Cutting Conditions	Wear Resistance test
Work Piece	SCM435(260 HB)
Cutting Velocity, m/min.	150
Feed,mm/min.	0.36
Depth of cut, mm	1.5
Condition	Wet

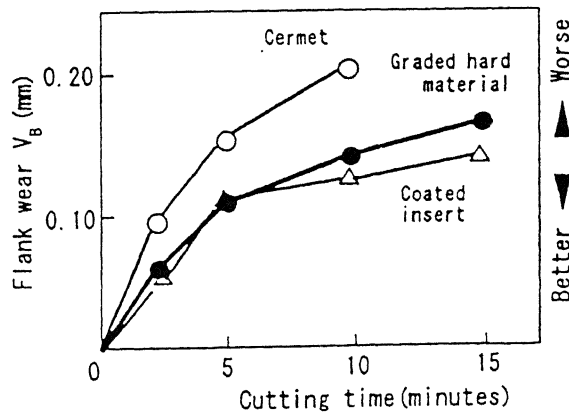Table 2.3: Cutting Conditions in Wear Resistance tests

Figure 2.10: Results of Cutting Wear Resistance tests

2.9 Design of FGM

The design of an FGM must be conducted by taking into account the conditions it will encounter in practical application. This involves an effort to select an optimum material combination to ease heat stresses, an optimum inter material compositional distribution that is suitable for production conditions, and the optimum micro structures for the material involved. Figure2.11. shows the inverse design procedure employed by Mirano and associates [28] in their design effort.

The inverse design procedure works as follows:

1. Required shape and heat boundary conditions are set in developing an FGM structure, and the selection of suitable materials and a production method is made by using the data base.

2. The selection of an optimum composition distribution function is made to control and to represent the required gradient material composition, and the profiles of the FGM are determined by setting parameters.

3. The selection of an inferred model of material properties is made based on the required microstructure of the FGM. This is achieved by obtaining data on the properties of the basic compositional materials involved from a material property data base. At the same time, the shape parameters of the mathematical model of the microstructure are determined. Using property values obtained from an arbitrary material composition created by these processes, the analysis of the temperature distribution and thermal stress distribution are conducted.

4. An effort is made to derive a compositional distributional profile, and an optimum material combination to minimize the specific stress(stress/material strength) by adjusting gradient distribution parameters and material combination.

Considering that these requirements involve repeated calculations to attain a global opti-

mization in basic design, a three dimensional analysis by FEM is not practical because of

its limitations in terms of analysis time. In addition a method for controlling three dimen-

sional compositional distribution has yet to be established. Under these circumstances, in

basic design state, it is important to make an effort to attain a one-dimensional optimum

compositional distribution in designing the basic shape of an FGM before two-dimensional

optimization becomes possible. At the same time in detailed design stage, an effort must

be made to analyze the non linear effects for material shapes that are practical use, to eval-

uate thermal fatigue strength, and to optimize localized compositional distribution data

obtained in the basic design.
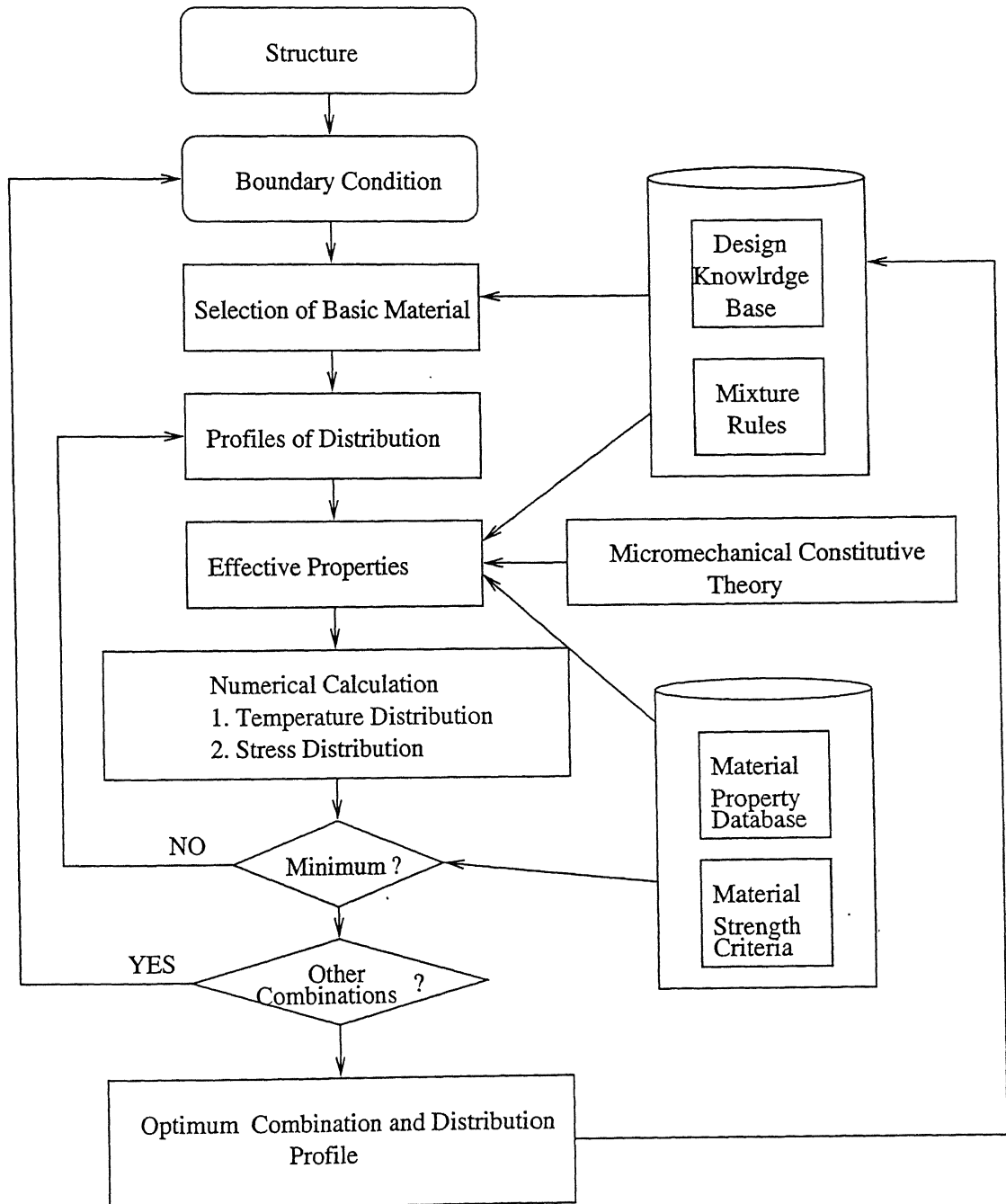
Figure 2.11: Inverse Design Procedure to Design an FGM

Chapter 3

Scope of The Present Work

The present study consists of preparing Ni-SiC functional gradient materials by a powder metallurgical route involving hot pressing of individual powder layer into an FGM compact, followed by sintering for further densification.

The physical and mechanical properties together with the microstructure of the sintered FGM compacts are also studied.

Chapter 4

Experimental Procedure

4.1 Raw Materials

4.1.1 Nickel Powder

In the present investigation carbonyl Nickel Powder supplied by INCO,U.K. was used.The Particle size distribution of the nickel powder is shown in Table-4.1 and in Fig-4.1. A typical SEM micro graph of the nickel powder is shown in Fig-4.2.

B. S. Sieve Number	wt%
+150	0.08
+200	1.562
+240	0.488
+300	2.735
+350	0.529
+400	2.856
+Pan	91.75

Table 4.1: Particle Size Distribution of Nickel Powder (Sieve Analysis)
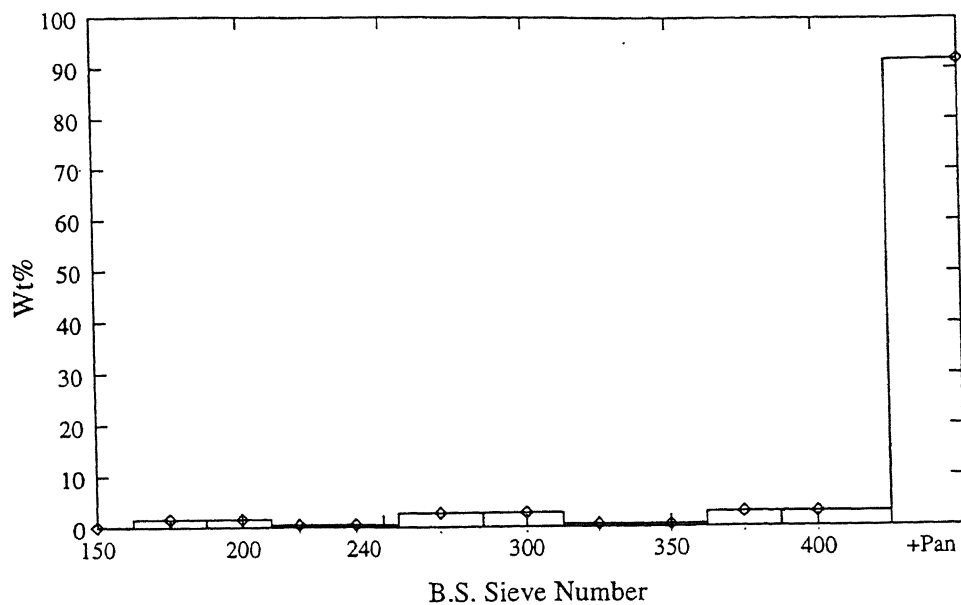
Figure 4.1: Particle Size Distribution of Nickel Powder
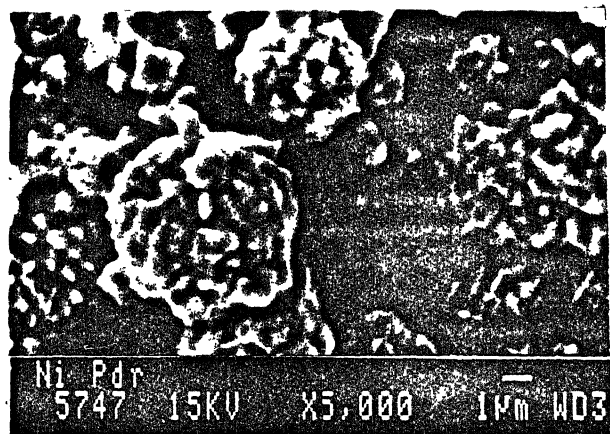
Figure 4.2: SEM photomicrograph of Nickel powder

4.1.2   Silicon Carbide Powder

In the present investigation particulate silicon carbide powders of size grit 1200 manufactured by Carborundum Ltd., was used. A typical SEM micrograph of the silicon carbide powder is shown in Fig.4.3.

Figure 4.3: SEM photomicrograph of SiC powder

4.2   Preparations of Powder Mixtures

Four batches of powder mixtures with varying percentage of Ni and SiC were prepared. The details of the compositions are as follows:

1. 1st batch - Ni - 50%, SiC - 50%

2. 2nd batch - Ni - 75%, SiC - 25%

3. 3rd batch - Ni -90%, SiC - 10%

4. 4th batch - Ni -100%, SiC -0%

PROCESS FLOW CHART

```
  ┌──────────────────────┐              ┌──────────────────────┐
  │  Carbonyl Ni Powder  │              │ Particulate SiC powder│
  └──────────────────────┘              └──────────────────────┘
              \                              /
               \                            /
                \                          /
                 ▼                        ▼
           ┌────────────────────────────────┐
           │            MIXING              │
           │ Carried out at a rotational    │
           │ speed of 30 rpm                │
           └────────────────────────────────┘
                          │
                          ▼
           ┌────────────────────────────────┐
           │         HOT PRESSING           │
           │ at temp. 950 deg C,            │
           │ Variables, Pressure 1 T, 2 T   │
           │ Time, 30 ,60,120 min.          │
           └────────────────────────────────┘
                          │
                          ▼
           ┌────────────────────────────────┐
           │          SINTERING             │
           │ at temp. 1050 ,1150 deg. C     │
           │ for 30, 60, 120 min.           │
           └────────────────────────────────┘
              /           │           \
             ▼            ▼            ▼
        ┌─────────┐  ┌─────────┐  ┌──────────────────┐
        │   SEM   │  │  EPMA   │  │  MICRO HARDNESS  │
        └─────────┘  └─────────┘  └──────────────────┘
```
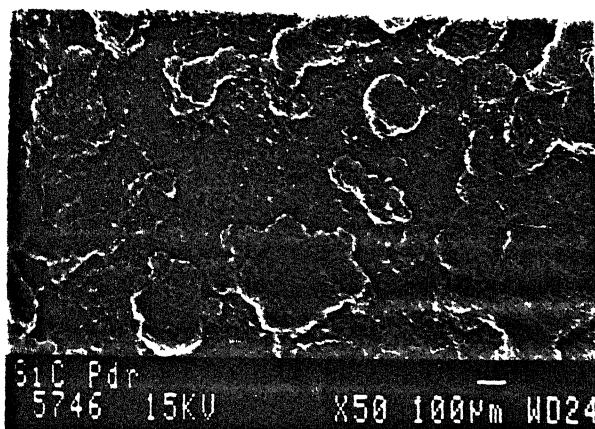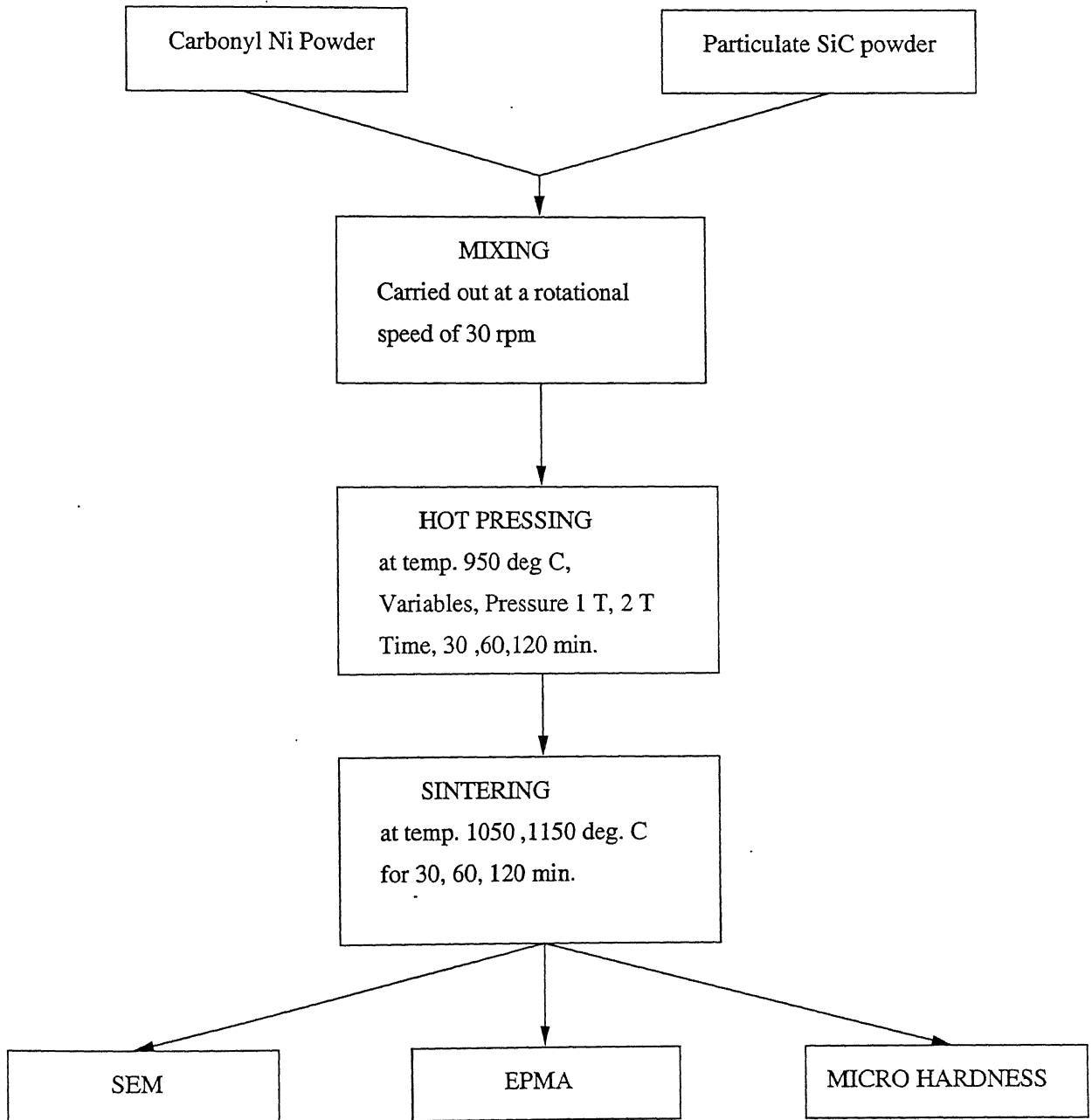
Figure 4.4: Powder Metallurgy Processing Schedule

The above powder mixtures were milled in a "Fritsh Pulverisette -5" Planetary Ball mill using tungsten carbide balls of 30 mm diameter in acetone medium for 24 hours, in order to prevent excessive heating and fusing of the particles.

4.3 Preparation of Ni-SiC FGM Compacts by Hot Pressing

The Ni-SiC FGM compacts were prepared by using a hot press, manufactured by the Electro fuel Manufacturing Co. Ltd.,Canada. The Press assembly consists of a precision post-and-platen press, a hydraulic cylinder, and air powered hydraulic system with electrical controls. The moving water cooled ram was accurately set perpendicular to the upper platen face, while the lower stationary water-cooled base was set parallel to the lower platen face.The hydraulic system was powered by compressed air. The required hydraulic pressure was set by using a pressure regulator mounted in the control panel. As the air motor cycles,the hydraulic motor fluctuates slightly around the set pressure. These slight periodic pressure variations have been found to be very effective in promoting densification in many cases. The modular heating unit uses molybdenum disilicide(super kanthal 33+) as heating elements and rests on the power connection legs. The heating unit is powered by an SCR power controller through a step down transformer. The programmable temperature controller compares the measured temperature(from the thermo couple) to the programmed set point and request the correct power level from the SCR power controller. The thermocouple, a chromel-Alumel type, is used to measure and control the temperature.

A graphite die of 25.5 mm inner diameter was specially prepared for making these compacts. After cleaning the die and punches,four layers of powder were poured in the die one by one. After one layered poured in the die and it was made uniform by applying the pressure with hand on the upper punch. Uniform filling will give more uniform finished

parts. The details of four layers of powder which were poured in the die are given in Table 4.2.

Table 4.2: Pouring Sequence of Powder in the die during Hot Pressing

Layer No from the bottom	wt of mixture, gm	Composition of mixture,%
I	2.50	50%Ni, 50% SiC
II	2.50	75% Ni, 25% SiC
III	2.50	90%Ni, 10% SiC
IV	2.50	100%Ni, 0%SiC

The filled die was then introduced in to the furnace of the hot press and was positioned under the hydraulic ram. A schematic diagram of hot press is shown in Fig.4.5. Hot pressing was carried out at temperature of $950°C$. The variables selected in the process of hot pressing were pressure(load) and time. The samples were prepared at a load of either one ton or two tons and at a soaking time of 30 minutes, 60 minutes or 120 minutes.

The variables selected during hot pressing were given in the Table 4.3.

Temp. $°C$,	Pressure, ton	Time, min.
950	1	30
950	1	60
950	1	120
950	2	30
950	2	60
950	2	120

Table 4.3: Parameters Studied during Hot Pressing

4.4 Sintering of Hot Pressed Ni-SiC FGM Compacts

Hot pressed compacts were further sintered at higher temperatures. Sintering experiments were carried out in a laboratory type silicon carbide resistance heated tubular furnace using a temperature programmer INDOTHERM "457" so as to achieve heating and cooling rates.
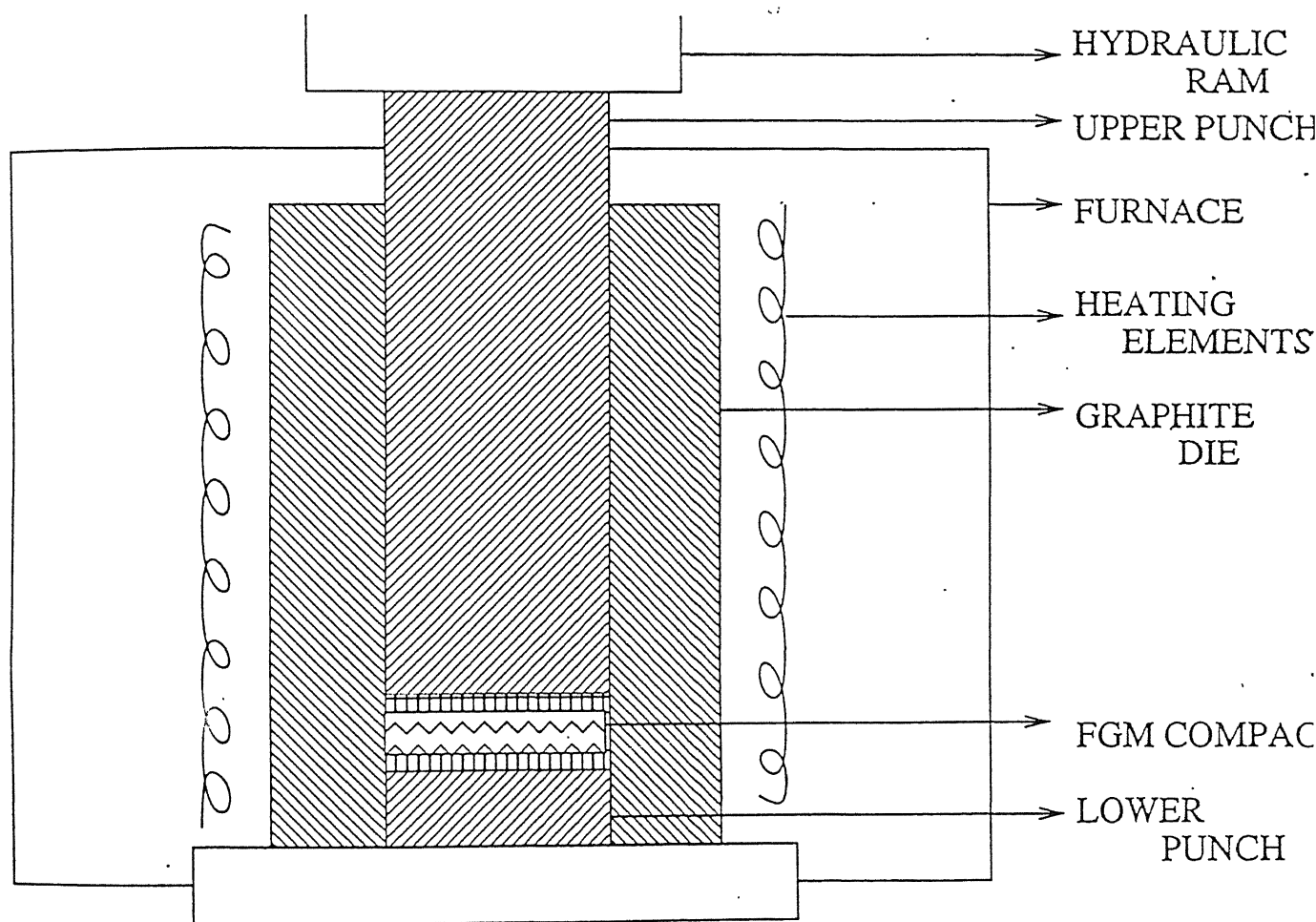
Figure 4.5: Hot Pressing Arrangement

The furnace tube had an internal diameter of 52 mm and capable of attaining a maximum temperature of 1400 °C with a control of 5 °C over a length of 100 mm at the center. Dry hydrogen was used as sintering atmosphere. The gas was allowed to pass through the lactro dryer containing activated Al_2O_3 for purification before finally passing through the furnace. The rate of gas flow was controlled by the gas regulator and it's flow was observed through the water bubbler for consistency before allowing to go out in the open atmosphere.

The sintering temperatures selected were 1050 °C and 1150 °C, While sintering period were 30 minutes, 60 minutes and 120 minutes.

Densities of "hot-pressed(hp)" and "hot-pressed sintered(hps)" compacts were calculated from the mass and dimensional measurements of the samples.

The xylene impregnation method was also used to measure the density values, and a difference of less than 5% was observed in densities measured by these two methods.

Following formula was used to calculate the density by the impregnation method.

Density of the compact= $Mass_{\{air\}}/[Mass_{\{imair\}} - Mass_{\{imwater\}}]$

Where,

$Mass_{\{air\}}$= Mass of the compact in air

$Mass_{\{imair\}}$= Mass of the xylene impregnated compact in air

$Mass_{\{imwater\}}$= Mass of the xylene impregnated compact in water

Densification parameter (ΔD) can be expressed as :

$$\Delta D = [D_{\{hps\}} - D_{\{hp\}}]/[D_{\{th\}} - D_{\{hp\}}]$$

Where,

$D_{\{hps\}}$= Density of hot pressed and sintered compact

$D_{\{hp\}}$= Density of hot pressed compact

$D_{\{th\}}$= Theoretical density of Ni-SiC (FGM) compact

Theoretical density of FGM compact was calculated from the mixture rule taking into

account the theoretical density values of individual components(See Appendix-1).

4.5 Characterization Methods

4.5.1 Sieve Analysis

Different metal powders used in the present study were characterized for particle size distribution by standard sieve analysis technique using the British standard(B.S) sieves.

4.5.2 Scanning Electron Microscopy

The powder samples for scanning electron microscopy were prepared by dispersion technique on a smooth substrate on which particles were spread with the help of methanol drying. The scanning photographs of the powder sample were taken under JEOL JSM 840A, scanning electron microscope(SEM).

SEM metallographic technique was adopted to study the microstructural changes of different layers of each compact.

4.5.3 Electron Micro Probe Analysis

Electron micro probe analysis was conducted on a JEOL SUPER PROBE JXA 8600 MX, Electron micro probe analyzer. Nickel concentration profile was obtained for the compact which was sintered at $1150°C$ for 120 min.

About three points were taken on each layer, and for each point average of three readings were taken. And nickel concentration profile of the compact which was sintered for maximum temperature and time was draw

4.5.4   Micro Hardness Testing

Micro hardness of sintered hot pressed compacts was measured in a LEITZ MINI LOAD-2 micro hardness tester for hardness profiles. 50 mN load was applied for the indentation purpose and the hardness was expressed in terms of HV (Vicker's hardness) scale of hardness. In each layer, hardness values were measured at three different locations, viz. two locations near the two interfaces/surfaces and one location at the middle of the layer. For each location, three measurements in the direction parallel to the interface/surface were taken and an average was calculated. From the data thus obtained, the hardness profile across all the layers of the Ni-Sic FGM compacts was drawn.

4.5.5   Density Measurement

Density of the hot pressed and sintered Ni-SiC FGM was measured by displacement method using Archimedes principle.

Chapter 5

Results And Discussion

5.1 Characterization of Hot Pressed Ni-SiC FGM Compacts

Hot pressing of Ni-SiC FGM compacts was done at a temperature of 950 $°C$, at soaking times of 60 min. and 120 min. Hot pressed FGM compacts were good. There was no spalling of layers. No crack was visible on the surface of the compacts. The effect of soaking time during hot pressing at 950 $°C$ on the density of Ni-SiC FGM compact is shown in Table 5.1.

Temp, $°C$	Time, min.	Density, gm/cc
950	60	4.98
950	120	5.25

Table 5.1: Density of hot pressed Ni-SiC FGM at different time

Even though the density of the FGM compacts increased with increase in the soaking time, the maximum density obtained during hot pressing after 120 min. was 5.25 gm /cc, which is about 82% of the theoretical value. Since the hot press used in the present study can operate at a maximum temperature of 950 $°C$, it was decided to further sinter the

FGM compacts at a higher temperature.

5.2 Characterization of Hot Pressed and Sintered Ni-SiC FGM Compacts

5.2.1 Density

The variation in the density of Ni-SiC FGM compacts with sintering time at 1150 $^{\circ}C$ sintering temperature is shown in the Figure 5.1. As it can be observed the density of the compact increases with sintering time. However, the rate of increase in density after 60 minutes sintering time is slightly more than before this time.

The density of the compact after sintering at 1150 $^{\circ}C$ for 120 minutes is 6.11 gm/cc, which is about 95% of the theoretical value. The theoretical density of the compact was calculated by using the mixture rule(See Appendix-1).

The reason for the low densification is attributed to the low values of the hot pressing temperature and pressure, and also low sintering temperature. Still higher densities may be achieved by increasing the temperature and pressure during hot pressing. Further increase in temperature during sintering would also help in increasing the density.

5.2.2 Densification Parameter

The variation of densification parameter of the sintered compact with respect to sintering period at 1150 $^{\circ}C$ is shown in Figure5.2. It can be seen from the figure that the densification parameter increases with increase in the sintering time. The densification parameter increases more rapidly beyond 60 minutes sintering time than before this time.

It can be seen that a densification parameter of about 0.73 was obtained for sintering time of 120 min. at 1150 $^{\circ}C$.
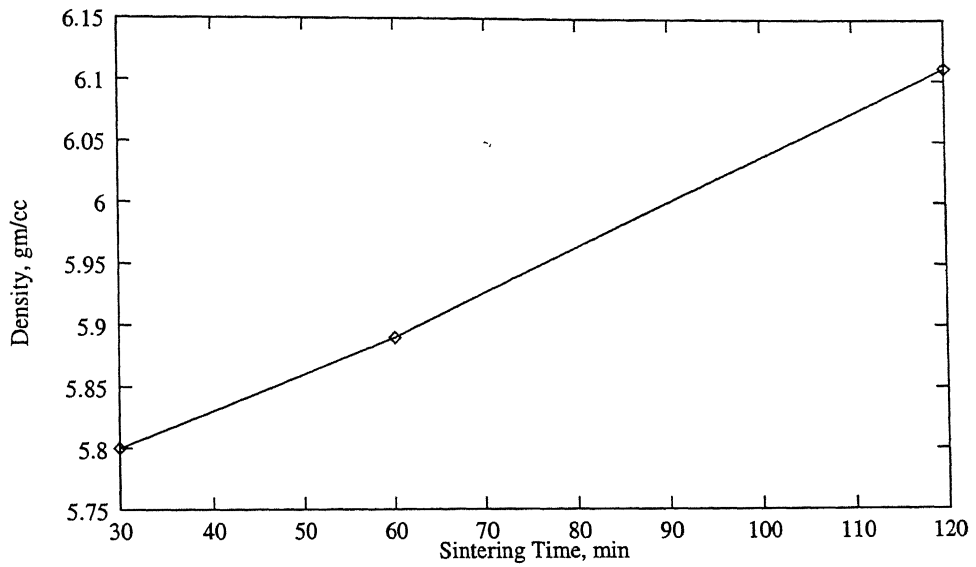
Figure 5.1: Variation in the density of Ni-SiC FGM compacts with sintering time
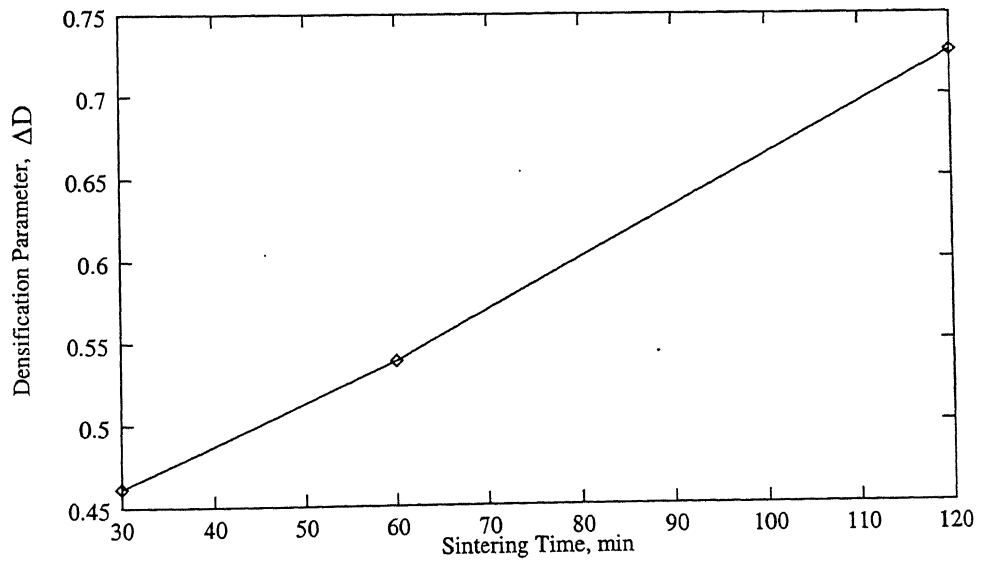

Figure 5.2: Variation of densification parameter with sintering time of sintered Ni-SiC FGM compact

5.2.3 Nickel Concentration Profile

Nickel concentration profile of hot pressed Ni-SiC FGM compact after sintering at 1150 °C for 120 min. is shown in the Fig.5.3. The nickel concentration profile in the graded structure was characterized by using micro probe analysis. Micro probe analysis was performed to determine the distribution of the nickel from one surface to other surface.
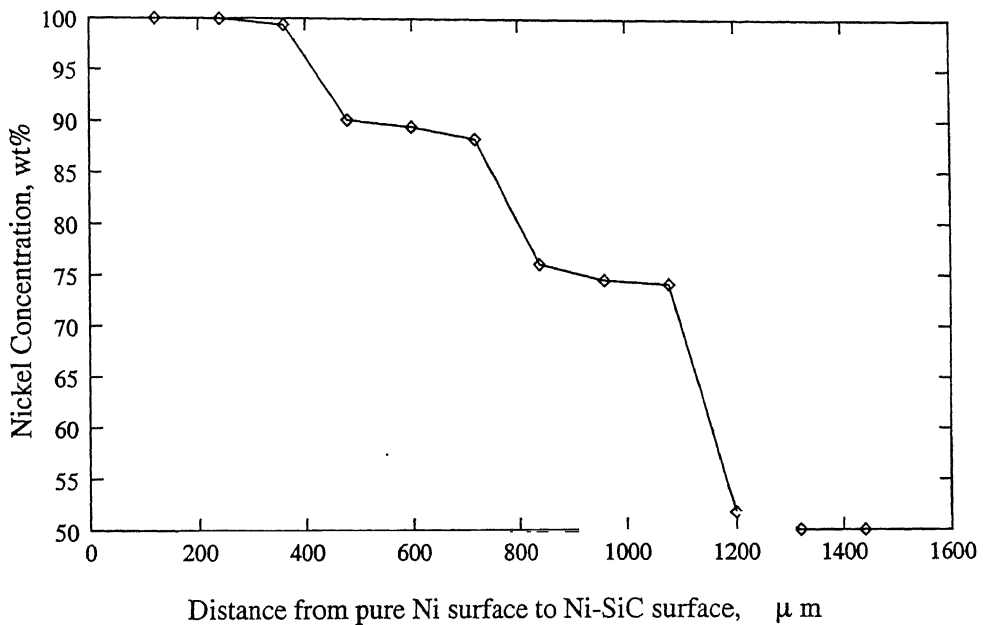
Figure 5.3: Nickel Concentration Profile

There are four layers in the Ni-SiC FGM compact. In the first layer 100 wt% nickel was taken, but after hot pressing and subsequent sintering it can be seen from the Fig.5.3, that the wt% of nickel is decreases from 100% on one side to 99.8% to other side of the layer. It is apparent that very little diffusion of nickel from the first layer (containing 100% Ni) to the second layer (containing 90% Ni and 10% SiC) has taken place. In the second layer 90 wt% nickel was taken , but after hot pressing and sintering the wt% of nickel is decreasing from 90.1% on one side to 88.3% on the other side of the second layer. It is evident that the nickel concentration in the second layer at area adjacent to the first layer (containing 100% Ni) has not increased to any significant level, but there is a greater decrease in the

nickel content at the area adjacent to the third layer (containing 75% nickel and 25% SiC). This suggests that more nickel has diffused from the area in the second layer near (90% nickel, 10% SiC)/(75% Ni,25% SiC) interface. Also, the nickel concentration in the second layer is continuously decreasing from the 100% nickel/(90% nickel, 10% SiC) interface to the (90% nickel, 10% SiC)/(75% nickel, 25% SiC) interface. Similarly in the third and fourth layer the wt% of nickel are 75% and 50% respectively. But in this case also after hot pressing and sintering it can be seen that the wt% of nickel in the third layer is from 76% on one side to 74% on the other side of the third layer. The behaviour is similar to that observed in the second layer. The respective values of the fourth layer were 51.7% nickel on one side to 50.8% nickel on the other side of the layer. The nickel content in the entire fourth layer has increased from its original value of 50%. Obviously, the increase in nickel content is more near the (75% Ni, 25% SiC)/(50% Ni,50% SiC) interface than on the free surface. The nickel content in the entire fourth layer has increased from it's original value of 50%. Obviously, the increase in nickel content is more near the (75% Ni, 25%SiC)/(50%Ni,50%SiC) interface than on the free surface of the fourth layer.

It is evident that there are some minor changes in the nickel concentration in all the four layers of the Ni-SiC FGM compacts. The changes are not uniform in each layer. Nevertheless, it can be concluded that no homogenization of any significance was observed in the Ni-SiC FGM compacts after final sintering at $1150°C$ for 120 minutes.

5.2.4 Micro Hardness Profiles:

The micro hardness values were measured across the cross-section near the edge of the Ni-SiC FGM compact sintered for 60 min. and 120 min. at a temperature of $1050°C$, and for 60 min. and 120 min. at a temperature of $1150 °C$. For each measurement an average of three readings were taken.

The comparison of the hardness value of the each layer sintered Ni-SiC FGM compacts

obtained after sintering at different temperature and time is shown in Fig.5.4- 5.7.

Fig.5.4 and 5.5 show the comparison of micro hardness of Ni-SiC FGM compacts sintered for 60 min. and 120 min. at temperature of 1050 °C, and for 60 min. and 120 min. at temperature of 1150 °C respectively.

It can be seen that as we move from pure nickel surface (100% Ni, 0% SiC) from one side to the (50% Ni,50% SiC) surface on the other side the hardness value increases. It is obvious that the increase in hardness value is due to the increasing amount of hard SiC phase in the successive layers. Further, the hardness of each layer is more for sintering time of 120 min. than for 60 min. both at sintering temperature of 1050°C and 1150°C. Obviously the increase in hardness with increase in time is due to higher amount of densification. It is obvious that the increase in hardness value is due to the higher amount of sintering with increase in time.

Fig.5.6 and 5.7 show the comparison of micro hardness of Ni-SiC FGM compacts sintered at temperatures of 1050°C, and 1150°C for 60 min., and at temperatures of 1050°C and 1150°C for 120 min. sintering time respectively.

It can be seen from the Fig.5.6 and 5.7 that as we increase sintering time from 60 min.to 120 min.the change in micro hardness with temperature increases.

5.3   Microstructural Investigation

The SEM photomicrograph of Ni-SiC FGM compacts at various layers and interfaces are shown in Fig.5.8 to 5.12. Fig.5.8(a),(b),(c) and (d) show the microstructures of 100% Ni, 90% Ni-10% SiC, 75% Ni-25% SiC and 50% Ni-50% SiC layers of Ni-SiC FGM compact sintered for 60 min. at 1050 °C in hydrogen respectively.

Fig.5.9(a),(b),(c) show the microstructures of interface of 100% Ni and 90% Ni-10% SiC layers, 90% Ni-10% SiC and 75% Ni-25% SiC layers, and 75% Ni-25% SiC, and 50%
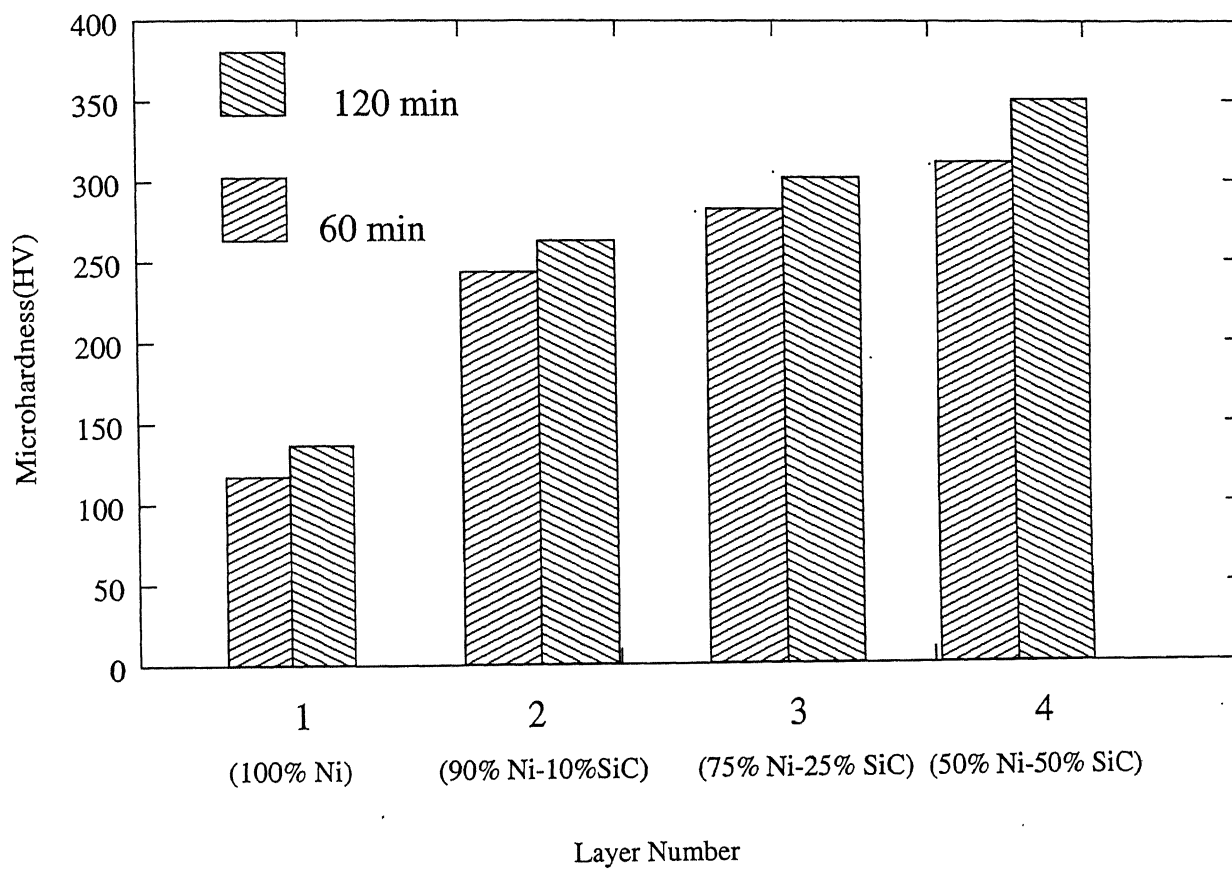
Figure 5.4: Comparison of Micro hardness of Ni-SiC FGM Compact Sintered for 60 min, 120 min at $1050°C$
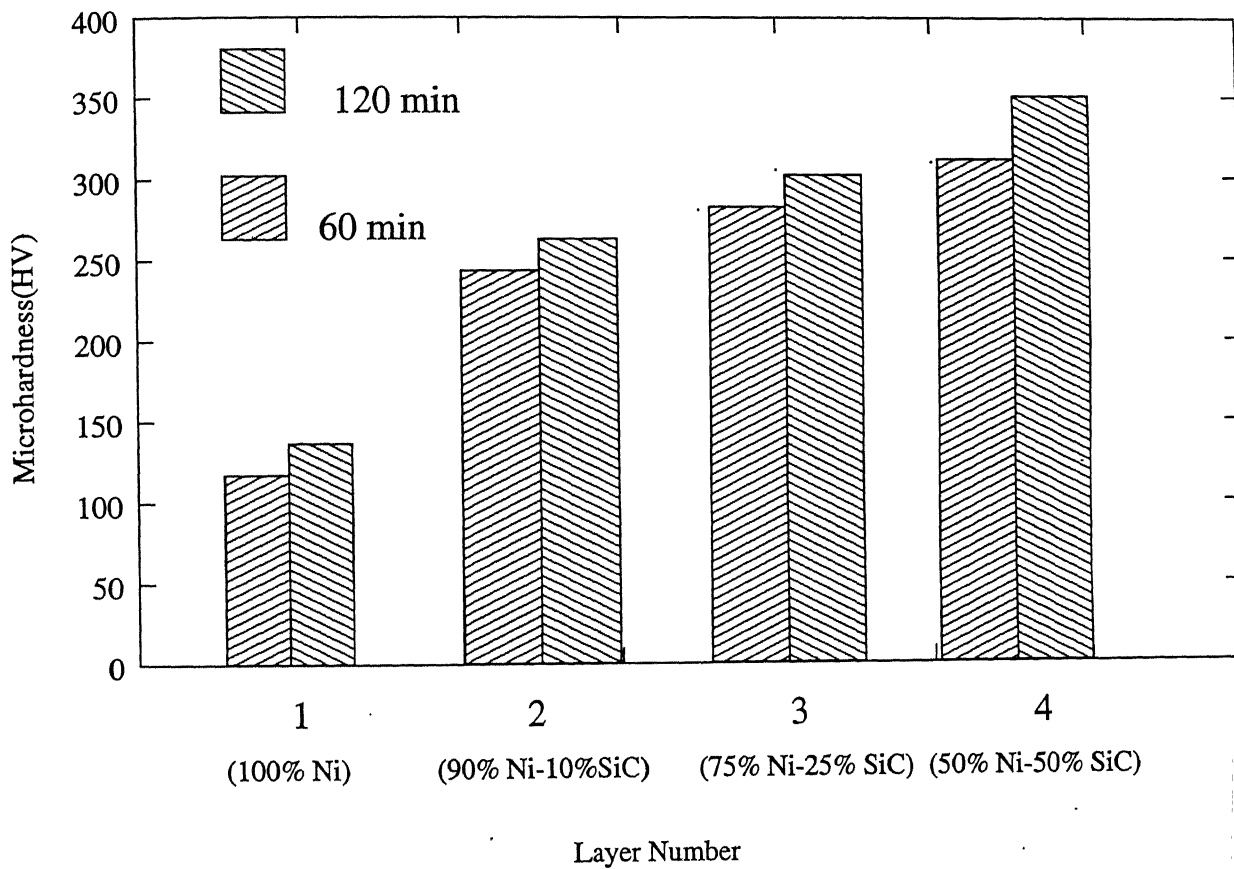
Figure 5.5: Comparison of Micro hardness of Ni-SiC FGM Compact Sintered for 60 min. and 120 min. at 1150°C
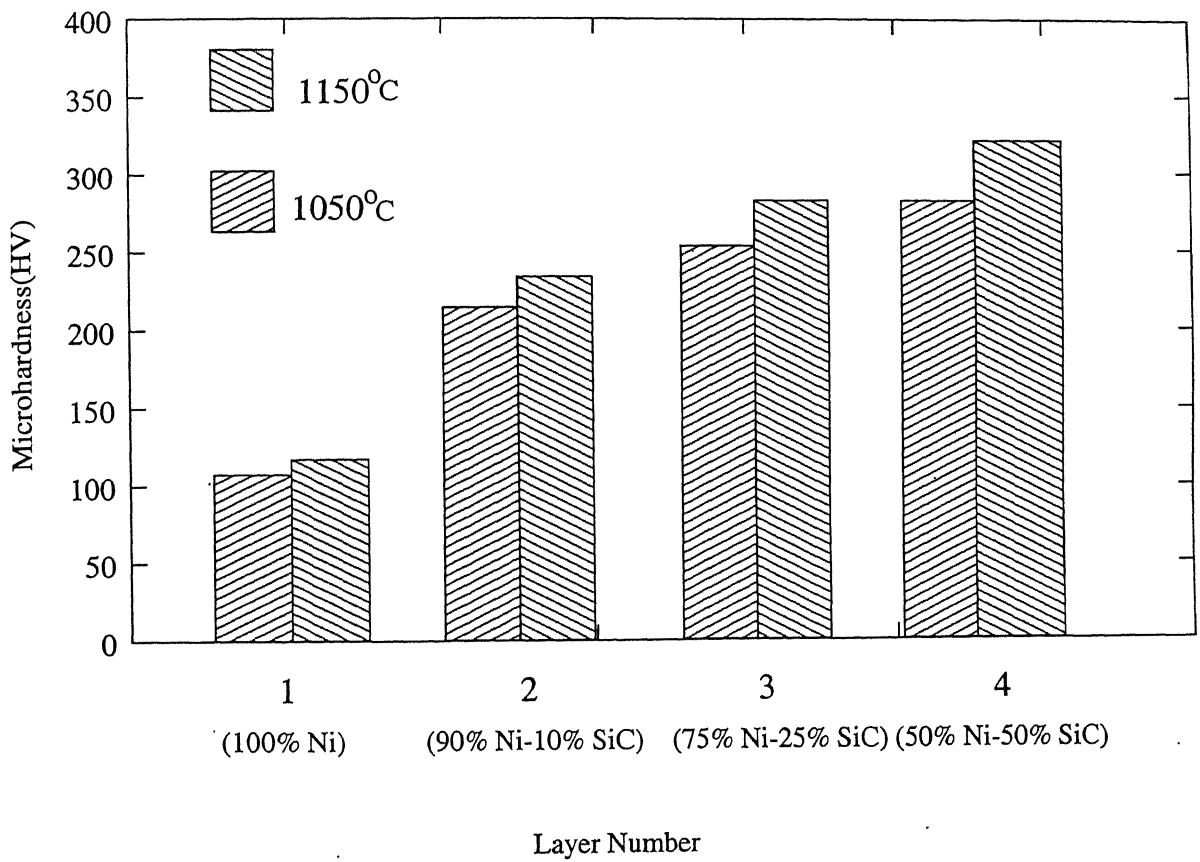
Figure 5.6: Comparison of Micro hardness of Ni-SiC FGM Compact sintered for 60 min. at temperature $1050°C$ and 60 min. at $1150°C$
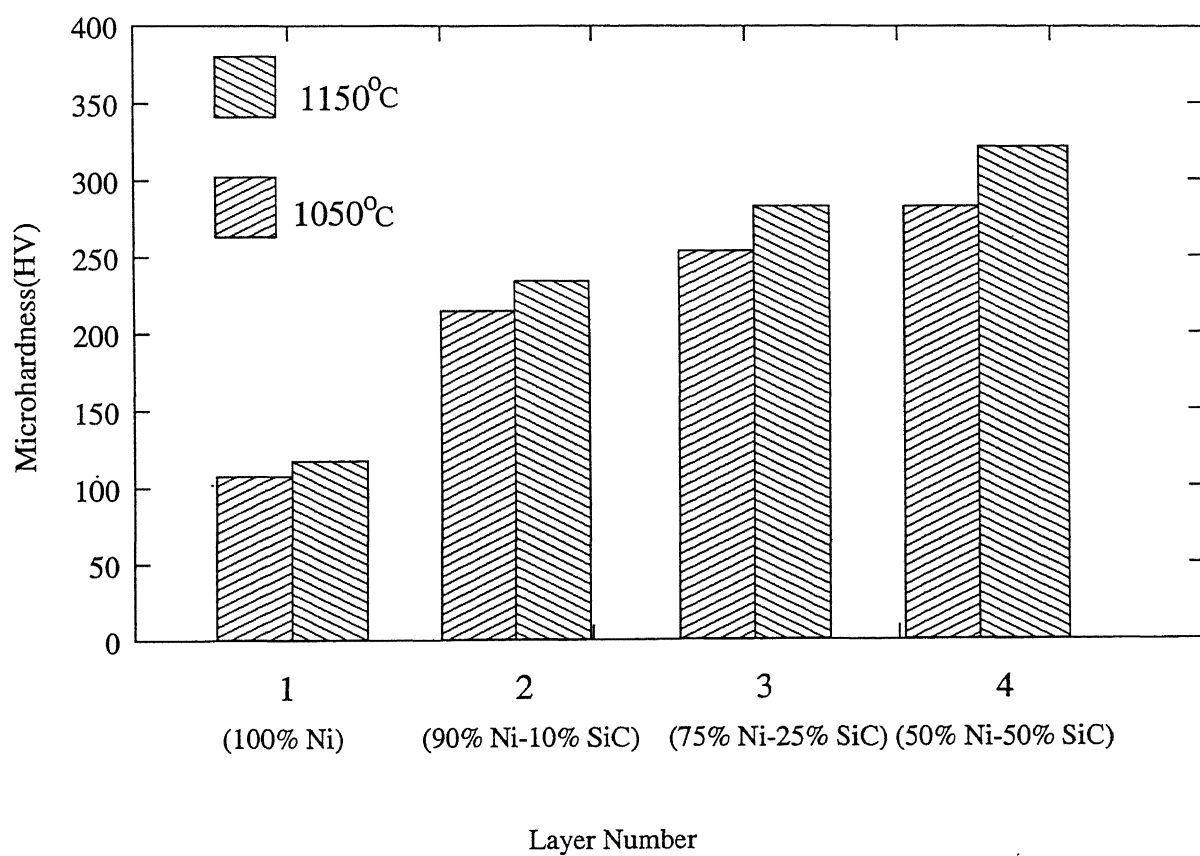
Figure 5.7: Comparison of Microhardness of Ni-SiC FGM Compact Sintered for 120 min. at temperature 1050°C and 120 min. at 1150°C

Ni-50% SiC layers of Ni-SiC FGM compact sintered for 60 min. at 1050 °C in hydrogen. Before sintering the compact was hot pressed for 60 min. at 950 °C.

It can be seen that from the Fig.5.8(a),(b),(c) and (d) that the homogeneity of SiC reinforcement is good, although some agglomerates of the finest SiC particles have formed. There is no indication of cracks in all the layers. Pores are small in size. Few large pores are also present which are evenly distributed.

It can be seen from the Figure 5.9(a),(b), and (c) that the interfaces between the layers are clearly visible. Adhesion between the layers is good. Mixing of layers close to the interfaces is not observed. Only in case of Figure 5.9(b) interface cracking is seen which may be due to development of residual stresses at the interface of two layers. However, there was no interface cracking in Fig.5.9(a) and 5.9(c).

Figure 5.10(a), (b), (c) and (d) show that the microstructures of 90% Ni- 10% SiC layer of Ni-SiC FGM compacts sintered at 1050 °C for 60 min., 1050 °C for 120 min.,1150°C for 60 min., and 1150 °C for 120 min. respectively. It can be seen from the Figure 5.10(a),(b) and 5.10(c),(d) that porosity is decreasing with sintering time and temperature.

Fig.5.11(a),(b),(c) and (d) show the microstructures of 75% Ni-25% SiC layer of Ni-SiC FGM compacts sintered at 1050 °C for 60 min., 1050 °C for 120 min.,1150 °C for 60 min., and 1150 °C for 120 min. respectively. It can also be seen from the Fig. 5.11(a),(b) and 5.11(c) (d) that the amount of pores is decreasing with sintering time and temperature.

Fig.5.12(a),(b) and (c) show the microstructures of interfaces of 100% Ni and 90% Ni-10% SiC, 90% Ni-10% SiC and 75% Ni-25% SiC and 75% Ni-25% SiC and 50% Ni-50% SiC layers of Ni-SiC FGM compact sintered for 120 min. at 1150 °C . It can be seen from the Fig.5.12(a),(b) and (c) that the interfaces are clearly visible. Some diffused layers are also present which may be due to diffusion of nickel from one layer to other. Band structure is also observed in the second layer near the 100% Ni/(90%Ni,10%SiC) interface. It is apparent that the microstructure discontinuity (100% Ni/ 90% Ni-10% SiC/ 75% Ni-25%
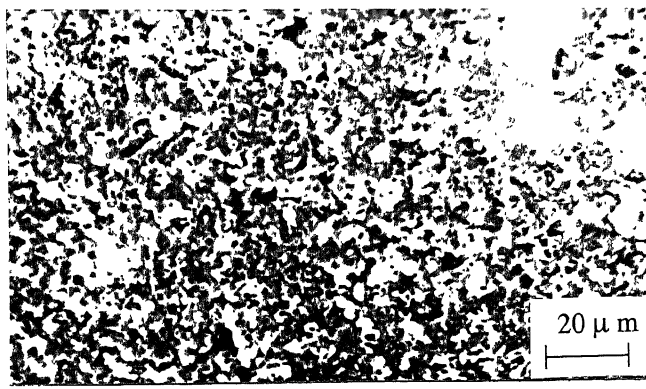
SiC/ 50% Ni-50% SiC) is stable after heating at 1150 $°C$ for 120 min., and homogenization has not taken place.
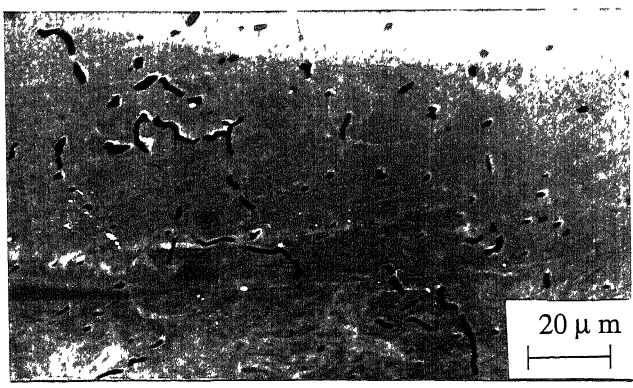
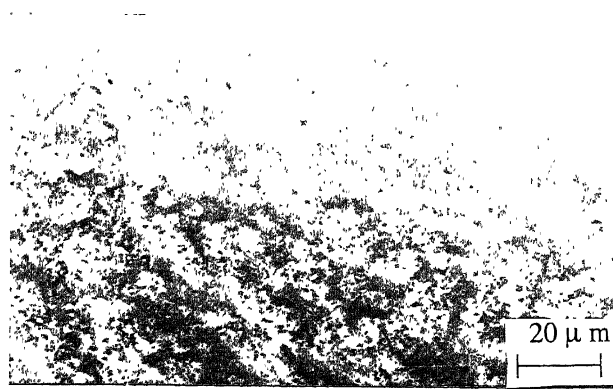(a) Layer containing 100 Ni
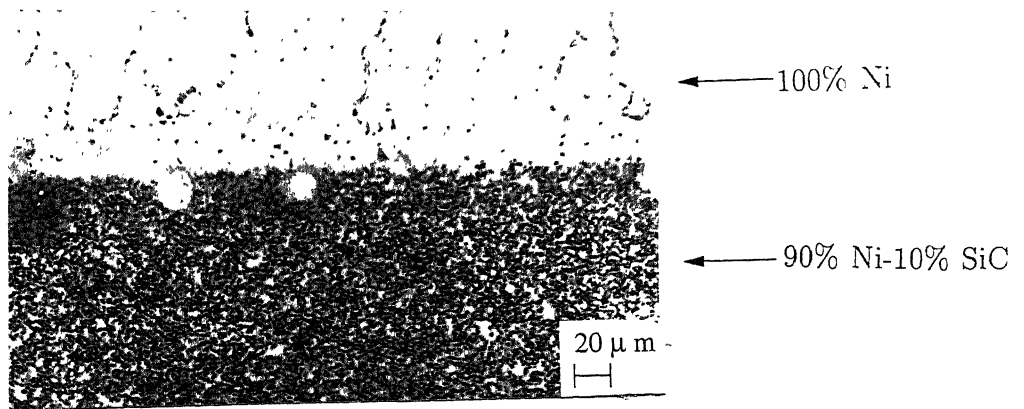

(b) Layer containing 90% Ni and 10% SiC
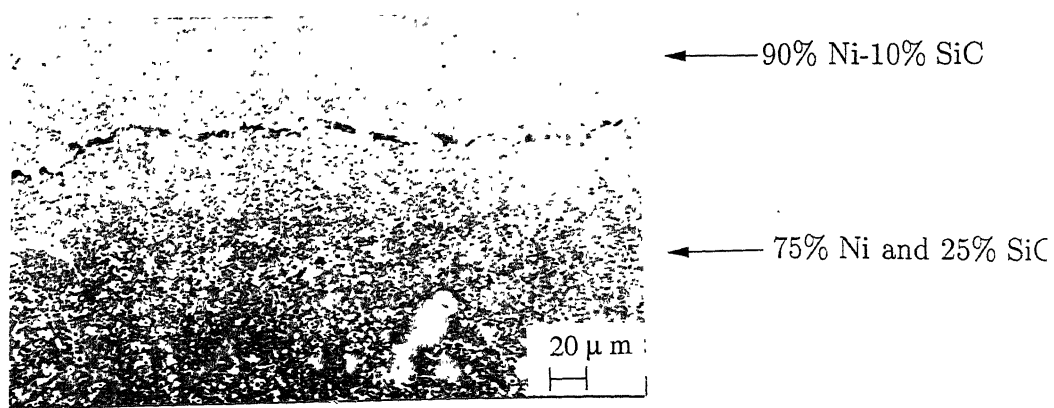

(c) Layer containing 75% Ni and 25% SiC

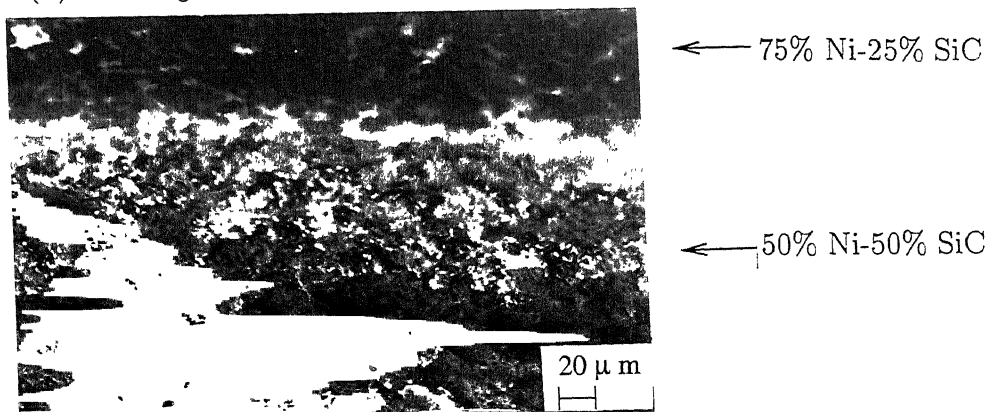(d) Layer containing 50% Ni and 50% Si

Fig.5.8:SEM Photomicrographs showing different layers of Ni-SiC(FGM) Sintered for 60 min. at 1050 degC.

(a) Showing interface of 100 Ni and 90% Ni-10% SiC layers

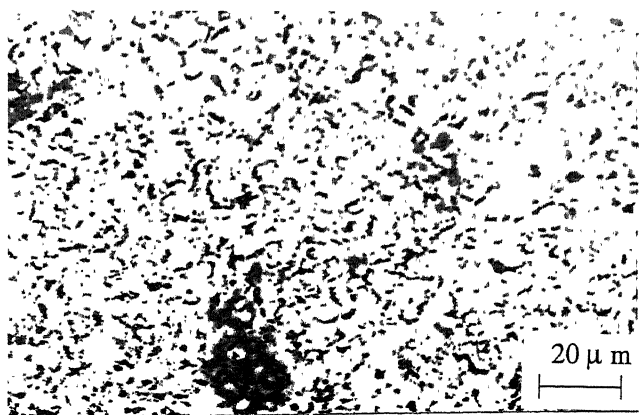(b) Showing interface of 90% Ni-10% SiC and 75% Ni-25% SiC layers

(c) Showing interface of 75% Ni-25% SiC and 50% Ni-50% SiC layers
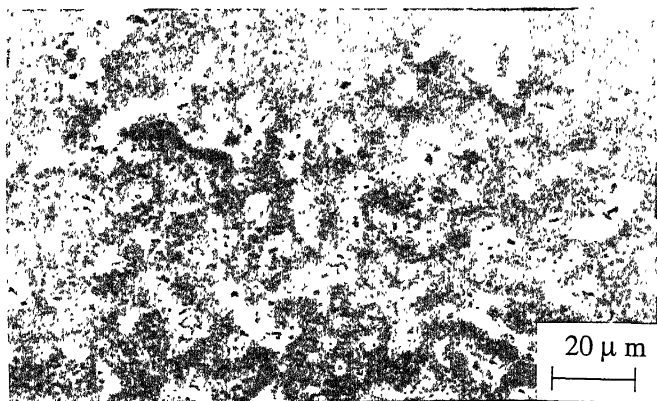
Fig.5.9:SEM photomicrographs showing different interfaces of Ni-SiC(FGM) Sintered for 60 min. at 1050 degC.
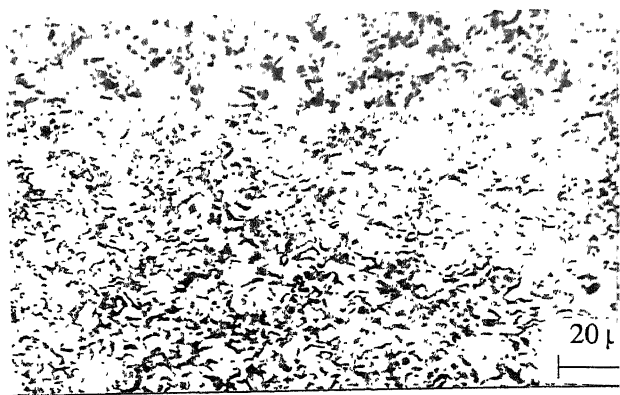
(a) Layers containing 90% Ni-10% SiC

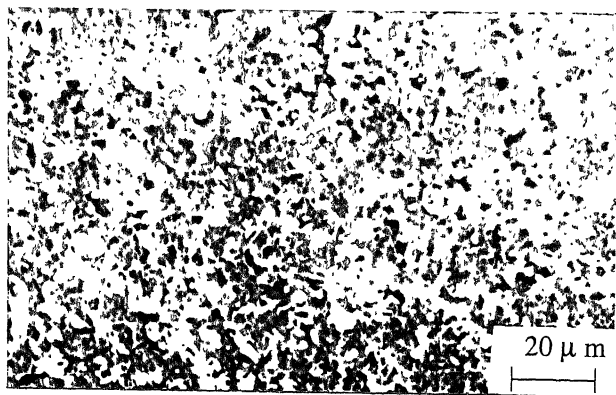(b) Layers containing 90% Ni-10% SiC

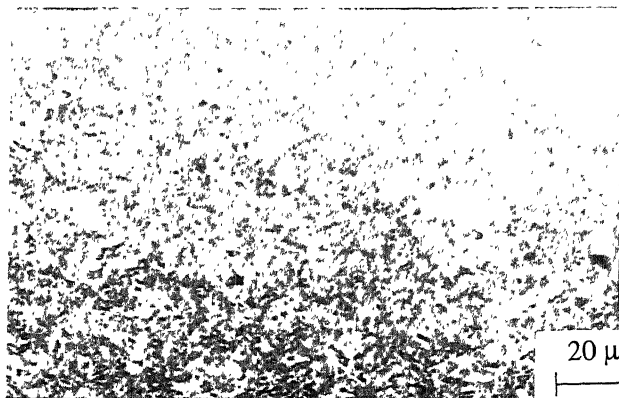(c) Layers containing 90% Ni-10% SiC

(d) Layers containing 90% Ni-10% SiC

Fig.5.10:SEM photomicrographs showing 90% Ni-10% SiC layer of different compacts sintered (a)for 60 min at 1050 degC (b)for 120 min. at 1050 degC (c)for 60 min. at 1150 degC (d)for 120 min at 1150 degC.
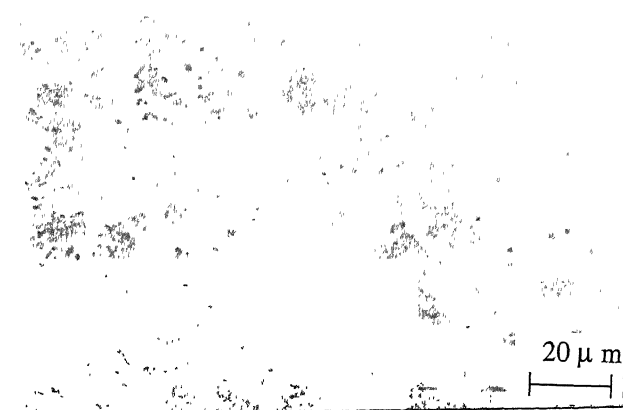
(a) Layer containing 75% Ni and 25% SiC

(b) Layer containing 75% Ni and 25% SiC

(c) Layer containing 75% Ni and 25% SiC

(d) Layer containing 75% Ni and 25% SiC

Fig.5.11:SEM photomicrographs showing 75% Ni-25% SiC layer of different compacts sintered (a) for 60 min. at 1050 degC. (b) for 120 min. at 1050 degC. (c) for 60 min. at 1150 degC. (d) for 120 min. at 1150 degC.
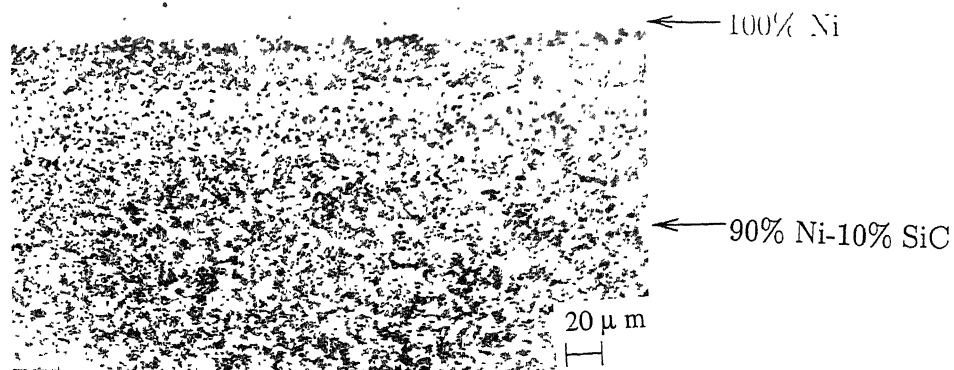
(a) Showing interface of 100 Ni and 90% Ni-10% SiC layers
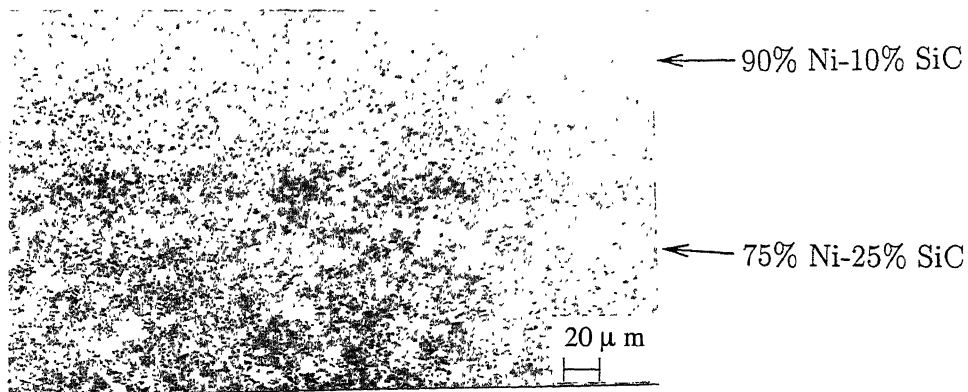
(b) Showing interface of 90% Ni-10% SiC and 75% Ni-25% SiC layers
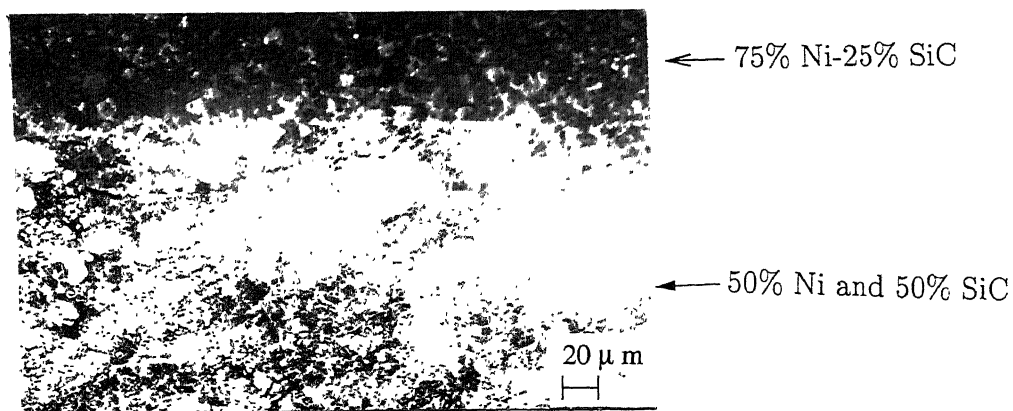
(c) Showing interface of 75% Ni-25% SiC and 50% Ni-50% SiC layers

Fig.5.12:SEM photomicrographs showing interfaces of Ni-SiC(FGM) compacts sintered for 120 min. at 1150 degC. X200

Chapter 6

Conclusions

1. Powder Metallurgy Ni-SiC FGM compacts consisting of four layers having composition 100% Ni, 90% Ni-10% SiC, 75% Ni-25% SiC and 50% Ni-50% SiC can successfully be formed by hot pressing at 950 °C. The hot pressed Ni-SiC FGM compacts has an apparent density equal to about 82% of the theoretical after hot pressing at 950 °C for 120 min.

2. Sintering of the above hot pressed four layer Ni-SiC FGM compacts 1150 °C for 120 min. increases the apparent density from 82 % to about 95% of the theoretical. Still higher densities can be achieved by increasing the sintering temperature.

3. The interface between the layers of the sintered Ni-SiC FGM compacts remains sharp.

4. From the Nickel concentration profile obtained by EPMA studies, it is evident that no noticeable homogenization of the Ni-SiC FGM compacts has taken place, after sintering at 1150°C for 120 min.

Chapter 7

Suggestion for Future Work

1. Ni-SiC FGM compacts having 100% Ni on one side and 100% SiC on the other side should be prepared and their properties should be investigated.

2. Hot isostatic pressing of the FGM compacts may be carried out for increased densification. For hot isostatic pressing the length/dia. ratio of the FGM compact should be greater than 1. In the present study the length/dia ratio of the FGM compact is about 0.2. Further work is needed in this direction.

Appendix

1. Calculation of Theoretical Density of Ni-SiC FGM Compact

The theoretical density of the Ni-SiC FGM compact is calculated by using the formula

$$\rho_{Ni-SiC} = \frac{W_{Ni} + W_{SiC}}{\frac{W_{Ni}}{\rho_{Ni}} + \frac{W_{SiC}}{\rho_{SiC}}} = \frac{\sum W_i}{\sum \frac{W_i}{\rho_i}} \tag{A.1}$$

where

ρ_{Ni-SiC} = Theoretical density of Ni-SiC,

W_i = Weight fraction of 'i' element,

ρ_i = Theoretical density of 'i' element.

In the present calculation W_{Ni}, W_{SiC}, ρ_{Ni}, ρ_{SiC} are taken to be 7.87 gms, 2.125 gms, 8.9 gm/cc and 3.1722 gm/cc respectively which yielded a theoretical density value of 6.43 gm/cc.

2. Hardness Values of Ni-SiC FGM Compact Sintered for 60 min., 120 min. at $1050°C$ and $1150°C$, which are Hot Pressed at 2 ton Load

Comparison of microhardness values of Ni-SiC FGM compact sintered for 60 min., and 120 min. at $1050°C$.

wt% of Ni and SiC	Hardness at time of 60 min.	Hardness value at time of 120 min.
100% Ni, 0% SiC	101.94	116.54
90% Ni, 10% SiC	207.24	227.85
75% Ni, 25% SiC	253.34	276.89
50% Ni, 50% SiC	283.0	315.37

Comparison of microhardness value of Ni-SiC FGM compact sintered for 60 min., and 120 min. at $1150°C$.

wt% of Ni and SiC	Hardness at time of 60 min.	Hardness value at time of 120 min.
100% Ni, 0% SiC	115.76	132.15
90% Ni, 10% SiC	238.2	262.17
75% Ni, 25% SiC	281.1	305.6
50% Ni, 50% SiC	310.44	343.8

Comparison of microhardness values of Ni-SiC FGM compact sintered for 60 min., at 1050°C and 1150°C.

wt% of Ni and SiC	Hardness at temp1050°C	Hardness value at temp.1150°C
100% Ni, 0% SiC	101.94	115.76
90% Ni, 10% SiC	207.24	238.2
75% Ni, 25% SiC	253.34	281.1
50% Ni, 50% SiC	283.0	310.44

Comparison of microhardness values of Ni-SiC FGM compact sintered for 120 min. at 1050°C and 1150°C.

wt% of Ni and SiC	Hardness at temp. 1050°C	Hardness value at temp.1150°C
100% Ni, 0% SiC	116.54	132.15
90% Ni, 10% SiC	227.85	262.17
75% Ni, 25% SiC	276.89	305.6
50% Ni, 50% SiC	315.37	343.8

3. Wt% Values of Nickel at Different Layer in the Nickel Concentration Profile of Ni-SiC FGM

Concentration values of Ni in wt% at different points from first to fourth layer of Ni-SiC FGM are shown below.

Distance from pure Ni surface to Ni-SiC surface in μm	Wt% of Ni
120	100.0
240	99.9
360	99.4
480	90.1
600	89.5
720	88.3
840	76.0
960	74.5
1080	74.0
1200	51.7
1320	50.0
1440	50.0

References

[1] K. Tsuda, A. Ikegaya, K. Isobe, N. Kitagawa, and T. Nomura: "Development of Functionally Graded Sintered Hard Materials", Powder Metallurgy, Vol.39, no.4, 1996, p.296-300.

[2] C.-Y. Lin, H.B. McShane, and R.D. Rawlings: "Structure and Properties of Functional Gradient Aluminum Alloy 2124/SiC Composites", Materials Science and Technology, Vol.10, no.7,1994, p.659.

[3] M. Sasaki and T. Hirani: "Fabrication and Properties of Functionally Gradient Materials", J. Ceram. Soc. Jap. 99, 1991, p.970-980.

[4] T. Hirai: "Functional Gradient Materials", Material Science and Technology, Vol.17B, 1996, p.293-341.

[5] M. Gasik: "Principles of Functional Gradient Materials and their Processing by Powder metallurgy", Acta Polytech. Scand., Ch 226, 1995.

[6] K. Atarashiya. "Joining Metals to Ceramics Using FGMs", Mater. and Proc. Rept., Hokkaido Univ., Mar/Apr 1992, Elssevier Sci. Publishing Co. Inc., p.5-6.

[7] "Improved Shuttle Tile", Aerospace Engr., June 1994, p.28.

[8] "Dental Implant Using Functionally Gradient Material", New Tech. JAPAN, JETRO, Vol. 20, no.11, Feb. 1993, p.17.

[9] "H. Takahashi: "Tohoku University Group Develops Moisture Absorbent/Proof Functionally Gradient Material", Sci. and Technol.: JAPAN, JPRS-JST-93-103-L, 52 pp., 21 , Dec. 1993, p.3.

[10] J.H. Abboud, R.D. Rawlings and D.R.F. West: "Functionally Gradient Layers of Ti-Al Based Alloys Produced by Laser Alloying and Cladding", Mater. Sci. and Technol., Vol.10, no.5, 1994, p.414-419.

[11] K. M. Jasim, R. D. Rawlings and D. R. F. West: "Metal-Ceramic Functionally Gradient Material Produced by Laser Alloying Processing", J. of Mater. Sci., Vol.28, 1993, p.2820-2826.

[12] Y. Kude: "FGMs via Chemical Vapor Deposition", Mater. and Proc. Rept., Nippon Oil Co., Ltd., Mar/Apr 1992, Elsevier Sci. Publishing Co. Inc., p.2-3.

[13] Partho Sarkar, Someswar Datta and Patrick S. Nicholson: "Electrophoretic Forming of Functionally-Graded Materials", J. Am. Ceram. Soc., Vol.76, no.4, 1997, p.15-19.

[14] Bernhard Ilschner: "Composition Gradient Materials", in 'Advances in Materials and their Applications', Ed. P. Rama Rao, Wiley Eastern Ltd., 1982, p.137-149.

[15] Y. Miyamoto: "Economic Process for Rapid Densification of Ceramics, Metals, and Functionally Gradient Materials", Processing Research Centre for High Performance Materials, Institute of Scientific and Industrial Research, Osaka Uni., Ibaraki. Osaka 567, Japan, VOl.8, no.5/6, May/June 1993, Mat. Tech., p.85-93.

[16] Y. Miyamoto: "Functionally Gradient Materials by SHS/HIP", JETRO, Vol.21, no.4,July 1993, p.30.

[17] H. J. Feng and J. J. Moore: "The Effect of Pressure on the Combustion Synthesis of a Functionally Graded Material: $TiB_2 - Al_2O_3 - Al$ Ceramic Metal Composite System", J. of Mater. Eng. and Performance, ASM Int., JMEPEG, Vol.2, no.5, Oct. 1993, p.645-650.

[18] H. Kimura and K. Toda: "Design and Development of Functionally Graded material by Pulse Dischar ge Resistance Consolidation with temperature Gradient Control",Powder Metallurgy, Vol.39, no.1,1996, p.59-62.

[19] H. Kimura and S. Kobayashi: Mater. Trans. JIM, Vol.36,1995, p.982

[20] H. Kimura and S. Kobayashi: J. JPN Inst. Met., Vol.58,1994, p.201

[21] H. Kimura and S. Kobayashi:"Inter metallic Compounds", J. JPN Inst. Met.,1991,p.985.

[22] C. Colin, L. Durant,N. Favort, J. Barbier and F. Delannay: "Processing of Functional Gradient WC-Co Cermet by Powder Metallurgy", Int. J. of Refractory and Hard Materials, Vol.12, 1993-94, p.145-152.

[23] A. Bishop, C.-Y. Lin, M. Navaratnam, et al."A Functionally Gradient Material Produced by a Powder Metallurgical Process", J. of Mater. Sci. Lett., Vol.12, no.19, 1993, p.1516-1518.

[24] "Functionally Gradient Material made of Glass and Metal", JETRO, New Tech. Japan, Vol.21, no.2, 1993.

[25] K. Morinaga and U. Kyushu: "Toto Fabricate Thick Alumina-Tungsten FGM Using Slip Cast Method", Sci. and Technol.: JPRS-JST-93-101-L, Dec. 1993, p.4.

[26] H. Takebe and K. Morinaga: " Fabrication of Zirconia-Nickel Functionally Gradient Materials by Slip Casting and Pressureless-Sintering", Materials and Manufacturing Processes, Vol.9, no.4, 1994, Marcel Dekker, Inc., p.721-733.

[27] "Supersonic Particle Process for Making Bulk Functionally Gradient Material", JETRO,New Tech. Japan, Vol. 21, no.7, 1993.

[28] T. Hirano, T. yamada and J. Teraki. Functionally Gradient Materials Symp., Sci. and Tech., Japan, JPRSS-JST-92-025, 2 Oct. 1992, p. 15-17 and 163. and "Fundamental Design, Multiobjective Optimization For FGM", Tokyo FGM '91, 1991, p.199-208.

A 127921